12. Tsavaris N, Kosmas C, Gouveris P et al (2004) Weekly gemcitabine for the treatment of biliary tract and gallbladder cancer. Invest New Drugs 22:193–198
13. Okusaka T, Ishii H, Funakoshi A et al (2006) Phase II study of single-agent gemcitabine in patients with advanced biliary tract cancer. Cancer Chemother Pharmacol 57:647–653
14. Hsu C, Shen YC, Yang CH et al (2004) Weekly gemcitabine plus 24-h infusion of high-dose 5-fluorouracil/leucovorin for locally advanced or metastatic carcinoma of the biliary tract. Br J Cancer 90:1715–1719
15. Alberts SR, Al-Khatib H, Mahoney MR et al (2005) Gemcitabine, 5-fluorouracil, and leucovorin in advanced biliary tract and gallbladder carcinoma: a North Central Cancer Treatment Group phase II trial. Cancer 103:111–118
16. Knox JJ, Hedley D, Oza A et al (2005) Combining gemcitabine and capecitabine in patients with advanced biliary cancer: a phase II trial. J Clin Oncol 23:2332–2338
17. Cho JY, Paik YH, Chang YS et al (2005) Capecitabine combined with gemcitabine (CapGem) as first-line treatment in patients with advanced/metastatic biliary tract carcinoma. Cancer 104:2753–2758
18. Doval DC, Sekhon JS, Gupta SK et al (2004) A phase II study of gemcitabine and cisplatin in chemotherapy-naive, unresectable gall bladder cancer. Br J Cancer 90:1516–1520
19. Thongprasert S, Napapan S, Charoentum C et al (2005) Phase II study of gemcitabine and cisplatin as first-line chemotherapy in inoperable biliary tract carcinoma. Ann Oncol 16:279–281
20. Andre T, Tournigand C, Rosmorduc O et al (2004) Gemcitabine combined with oxaliplatin (GEMOX) in advanced biliary tract adenocarcinoma: a GERCOR study. Ann Oncol 15:1339–1343
21. Kuhn R, Hribaschek A, Eichelmann K et al (2002) Outpatient therapy with gemcitabine and docetaxel for gallbladder, biliary, and cholangio-carcinomas. Invest New Drugs 20:351–356
22. McWilliams RR, Foster NR, Quevedo FJ et al (2007) NCCTG phase I/II trial (N9943) of gemcitabine and pemetrexed in patients with biliary tract or gallbladder carcinoma: phase II results. J Clin Oncol, Proc Am Soc Clin Oncol 25:217s (abstr 4578)
23. Fujii S, Ikenaka K, Fukushima M, Shirasaka T (1978) Effect of uracil and its derivatives on antitumor activity of 5-fluorouracil and 1-(2-tetrahydrofuryl)-5-fluorouracil. Jpn J Cancer Res (Gann) 69:763–772
24. Pazdur R, Lassere Y, Diaz-Canton E, Bready B, Ho DH (1996) Phase I trials of uracil-tegafur (UFT) using 5 and 28 day administration schedules: demonstration of schedule-dependent toxicities. Anticancer Drugs 7:728–733
25. Furuse J, Okusaka T, Funakoshi A, Yamao K, Nagase M, Ishii H et al (2006) Early phase II study of uracil-tegafur plus doxorubicin in patients with unresectable advanced biliary tract cancer. Jpn J Clin Oncol 36:552–556
26. Furuse J, Okusaka T, Boku N, Ohkawa S, Sawaki A, Masumoto T, Funakoshi A (2008) S-1 monotherapy as first-line treatment in patients with advanced biliary tract cancer: a multicenter phase II study. Cancer Chemother Pharmacol 62(5):849–855
27. Therasse P, Arbuck SG, Eisenhauer EA et al (2000) New guidelines to evaluate the response to treatment in solid tumors. European Organization for Research and Treatment of Cancer, National Cancer Institute of the United States, National Cancer Institute of Canada. J Natl Cancer Inst 92:205–216
28. Eckel F, Schmid RM (2007) Chemotherapy in advanced biliary tract carcinoma: a pooled analysis of clinical trials. Br J Cancer 96:896–902
29. Furuse J, Takada T, Miyazaki M et al (2008) Guidelines for chemotherapy of biliary tract and ampullary carcinomas. J Hepatobiliary Pancreat Surg 15:55–62
30. Yonemoto N, Furuse J, Okusaka T, Yamao K, Funakoshi A, Ohkawa S, Boku N, Tanaka K, Nagase M, Saisho H, Sato T (2007) A multi-center retrospective analysis of survival benefits of chemotherapy for unresectable biliary tract cancer. Jpn J Clin Oncol 37:843–851

Cancer Chemother Pharmacol (2009) 63:313–319
DOI 10.1007/s00280-008-0741-7

ORIGINAL ARTICLE

A phase II study of S-1 in gemcitabine-refractory metastatic pancreatic cancer

Chigusa Morizane · Takuji Okusaka · Junji Furuse · Hiroshi Ishii · Hideki Ueno · Masafumi Ikeda · Kohei Nakachi · Mina Najima · Takashi Ogura · Eiichiro Suzuki

Received: 27 December 2007 / Accepted: 11 March 2008 / Published online: 9 April 2008
© Springer-Verlag 2008

Abstract
Purpose Gemcitabine monotherapy or gemcitabine-containing combination chemotherapy is the standard first-line therapy for advanced pancreatic cancer. After disease progression, there is no standard regimen available. In a previous phase II trial, S-1 has been reported to show considerable efficacy, achieving a response rate of 37.5% in chemo-naïve patients with pancreatic cancer. This study evaluated the efficacy and toxicity of S-1 in patients with gemcitabine-refractory metastatic pancreatic cancer.
Methods Eligibility criteria were histologically proven pancreatic adenocarcinoma with confirmation of progressive disease while receiving gemcitabine-based first-line chemotherapy, 20–74 years of age, Karnofsky performance status of 80–100 points, with measurable metastatic lesions, adequate hematological, renal and liver functions, and written informed consent. S-1 was administered orally at 40 mg/m^2 twice daily for 28 days with a rest period of 14 days as one course. Administration was repeated until the appearance of disease progression or unacceptable toxicity. The primary endpoint of this study was an objective response, and secondary endpoints included toxicity, progression-free survival (PFS) and overall survival, as well as clinical benefit response in symptomatic patients.
Results Forty patients from two institutions were enrolled between September 2004 and November 2005. The most common adverse reactions were fatigue and anorexia, although most of those adverse reactions were tolerable and reversible. One patient developed grade 3 pneumonitis without neutropenia and recovered with appropriate antibiotic treatment. Although no complete response was seen, partial response was obtained in six patients (15, 95% confidence interval, 3.9–26%). Stable disease was noted in 17 patients (43%), and progressive disease in 15 patients (38%). Out of 19 evaluable patients, a clinical benefit response was observed in four patients (21%). The median PFS was 2.0 months, and the median survival time was 4.5 months with a 1-year survival rate of 14.1%.
Conclusion S-1 as monotherapy had marginal anti-tumor activity with tolerable toxicity in patients with gemcitabine refractory metastatic pancreatic cancer.

Keywords Chemotherapy · Pancreatic carcinoma · Second-line · Salvage

C. Morizane (✉) · T. Okusaka · H. Ueno · M. Ikeda · M. Najima · T. Ogura
Division of Hepatobiliary and Pancreatic Oncology, National Cancer Center Hospital, 5-1-1 Tsukiji, Chuo-ku, Tokyo 104-0045, Japan
e-mail: cmorizan@ncc.go.jp

J. Furuse · H. Ishii · K. Nakachi · E. Suzuki
Division of Hepatobiliary and Pancreatic Oncology, National Cancer Center Hospital, East, Kashiwa, Japan

Background

The prognosis of patients with pancreatic carcinoma is extremely poor because of difficulty in the early detection of this disease, the high incidence of postoperative recurrence, and ineffectiveness of nonsurgical treatments. Gemcitabine has been established as providing clinical benefit and a modest survival advantage over treatment with bolus 5-FU [3]. However, the benefit provided was inadequate, with an objective response rate of less than 15% and a median survival of 5–7 months. To improve the prognosis of patients with pancreatic cancer, one of the strategies is to develop the effective first-line chemotherapy including

gemcitabine combinations. Among various combinations with gemcitabine plus other agents as a first-line chemotherapy, only a few regimens have shown any survival benefit over single-agent gemcitabine [6, 20, 25], although the worldwide consensus regarding the results of these studies has not been established. Another strategy is to develop an effective second-line chemotherapy regimen after disease progression during first-line chemotherapy. However, despite the fact that several studies have investigated second-line chemotherapy in pancreatic cancer, the therapeutic results have been disappointing with poor response rate and survival [1, 2, 4, 5, 7, 14, 16, 18, 19, 21, 26, 27, 33, 34, 36, 38] Effective treatment in patients failing gemcitabine-based chemotherapy is eagerly awaited.

S-1 is a novel orally administered drug that is a combination of tegafur (FT), 5-chloro-2,4-dihydroxypyridine (CDHP), and oteracil potassium (Oxo) in a 1:0.4:1 molar concentration ratio [31]. CDHP is a competitive inhibitor of dihydropyrimidine dehydrogenase, which is involved in the degradation of 5-FU, and acts to maintain efficacious concentrations of 5-FU in plasma and tumor tissues [35]. Oxo, a competitive inhibitor of orotate phosphoribosyltransferase, inhibits the phosphorylation of 5-FU in the gastrointestinal tract, reducing the serious gastrointestinal toxicity associated with 5-FU [32]. The antitumour effect of S-1 has already been demonstrated in a variety of solid tumors such as advanced gastric cancer [15, 30], colorectal cancer [23], non-small-cell lung cancer [13], head and neck cancer [11], and breast cancer [29].

Concerning pancreatic cancer, a recent late phase II study of S-1 for chemo-naïve advanced pancreatic cancer patients demonstrated promising results with a response rate of 37.5% and a favorable toxicity profile [24]. Furthermore, clinical studies have reported activity of gemcitabine in pancreatic cancer patients with refractoriness to 5-FU [28], suggesting the lack of crossresistance between the gemcitabine and fluorinated pyrimidine, including S-1. Therefore, we conducted the present phase II study to investigate the feasibility and efficacy of S-1 in patients with advanced pancreatic adenocarcinoma in a progressive state under gemcitabine-based first-line chemotherapy.

Patients and methods

Patients

All patients were required to show histologically proven pancreatic adenocarcinoma with measurable metastatic lesions. Additional criteria included the following: progressive disease under gemcitabine-based first-line chemotherapy, post operative recurrence or metastatic disease before the start of first-line chemotherapy, 20–74 years of age, Karnofsky performance status (KPS) of 80–100 points, more than 3 weeks intervals between the last administration of the prior chemotherapy regimen and study entry, adequate bone marrow function (white blood cell count $\geq$ 3,000/mm^3, neutrophil count $\geq$ 1500/mm^3, platelet count $\geq$ 100,000/mm^3, haemoglobin level $\geq$ 9.0 g/dl), adequate renal function (serum creatinine level $\leq$ 1.5 mg/dL), and adequate liver function (serum total bilirubin level $\leq$ 2.0 mg/dL, transaminases level $\leq$ 2.5 times the upper limits of normal). Patients who had obstructive jaundice or liver metastasis were considered eligible if their transaminases levels could be reduced to within 5 times the upper normal limit of normal after biliary drainage. The exclusion criteria were as follows: regular use of phenytoin, warfarin or frucitocin, history of fluorinated pyrimidine use, severe mental disorder, active infection, ileus, interstitial pneumonia or pulmonary fibrosis, refractory diabetes mellitus, heart failure, renal failure, active gastric or duodenal ulcer, massive pleural or abdominal effusion, brain metastasis, active concomitant malignancy. Pregnant or lactating women were also excluded. Written informed consent was obtained from all patients. This study was approved by the institutional review board at the National Cancer Center in Japan.

Treatments

S-1 (Taiho Pharmaceutical Co., Ltd., Tokyo, Japan) was administered orally at a dose of 40 mg/m^2 twice daily after breakfast and dinner. Three initial doses were established according to the body surface area (BSA) as follows: BSA $<$ 1.25 m^2, 80 mg/day; 1.25 m^2 $\leq$ BSA $<$ 1.50 m^2, 100 mg/day; and 1.50 m^2 $\leq$ BSA, 120 mg/day. S-1 was administered at the respective dose for 28 days, followed by a 14-day rest period; this treatment course was repeated until the occurrence of disease progression, unacceptable toxicities, or the patient's refusal to continue. When a grade 3 or greater haematologic or grade 2 or greater nonhaeamatologic toxicity occurred, either the temporary interruption of the S-1 administrations until the toxicity decreased to grade 1 or less, or dose reduction by 20 mg/day (minimum dose, 80 mg/day) was recommended. If no toxicity occurred, the rest period was shortened to 7 days or the dose was gradually escalated in the next course (maximum dose, 150 mg/day), or both were permitted according to the judgment of the individual physicians. If a rest period of more than 28 days was required because of toxicity, the patient was withdrawn from the study. Patients were not allowed to receive concomitant radiation therapy, chemotherapy, or hormonal therapy during the study. Patients maintained a daily journal to record their intake of S-1 and any signs or symptoms that they experienced.

Response and toxicity evaluation

The response after each course was assessed according to the Response Evaluation Criteria in Solid Tumors (RECIST). Primary pancreatic lesions were not considered to be measurable lesions because the dimensions of such lesions are difficult to measure accurately. Physical examinations, complete blood cell counts, biochemistry tests, and urinalyses were performed at least weekly. Adverse events were evaluated according to the National Cancer Institute Common Toxicity Criteria, version 2.0.

Clinical benefit response

The clinical benefit response (CBR) was evaluated using the KPS and pain score, as described below [3]. The KPS was recorded weekly by the attending physician. Pain was evaluated by measuring the change from the baseline pain intensity and the daily dose of morphine or morphine-equivalent (doses of analgesic agents were converted to morphine-equivalent doses, i.e., 10 mg oxycodone = 15 mg morphine). The pain intensity was graded from 0 (no pain) to 100 (worst pain) using a visual analog scale and was recorded on a pain assessment card every day. Patients who fulfilled at least one of the following criteria were defined as eligible CBR analysis: (1) baseline pain intensity $\geq$20, or (2) baseline morphine consumption $\geq$10 mg/day. Moreover, all the patients underwent a 'pain stabilization period' for 2 days to ensure that the baseline values were stable before treatment: when the variation in the morphine consumption between 2 days was within 10 mg and the variation of the pain intensity was within 20, the patient was considered eligible for inclusion in the CBR analysis. For pain intensity, a positive response occurred when the score was improved by $\geq$50% from baseline, sustained for $\geq$4 weeks. For analgesic consumption, a positive response occurred when the weekly consumption was reduced by $\geq$50% from baseline, maintained for $\geq$4 weeks. A positive response for KPS was defined as an improvement of $\geq$20 points from baseline, sustained for at least 4 weeks. Any worsening from baseline, sustained for 4 weeks, was considered a negative response for each of the three domains. All the other results were considered stable. Pain intensity and analgesic consumption were compared to give a composite pain score. Each patient was classified positive, stable or negative for each of the primary measures (pain and KPS). In order to achieve a positive clinical benefit response, patients had to be positive for at least one parameter without being negative for any of the others for a minimum of 4 weeks. Patients who were stable in the two primary measures were classified as stable.

Statistical design

The primary endpoint of this study was objective response rate. The secondary endpoint of this study was clinical benefit response; toxicity; progression-free survival; and survival. The number of patients to be enrolled was planned using a SWOG's standard design (attained design) [8, 9]. The null hypothesis was that the overall response rate would be $\leq$5% and the alternative hypothesis was that the overall response rate would be $\geq$20%, the α error was 5% (one-tailed) and the β error was 10% (one-tailed). The alternative hypothesis was established based on the preferable data from previous reports [7, 16, 27, 36, 38]. Interim analysis was planned when 20 patients were enrolled. If none of the first 20 patients had a partial response or complete response, the study was to be ended. If a response was detected in any of the first 20 patients studied, an additional 20 patients were to be studied in a second stage of accrual to estimate more precisely the actual response rate. If the lower limit of the 90% confidence interval exceeded the 5% threshold (objective response in seven or more of the 40 patients), S-1 was judged to be effective and we would proceed to the next large-scale study.

The progression-free survival was calculated from the date of study entry to the date of documented disease progression or death due to any cause (whichever occurred first); and overall survival time was calculated from the date of study entry to the date of death or the last follow-up. The median probability of the survival period and progression-free survival were estimated using the Kaplan–Meier method. The relative dose intensity of S-1 was calculated according to the Hryniuk method [10].

Results

Patients

Forty consecutive patients with metastatic pancreatic cancer which was progressing under gemcitabine-based first-line chemotherapy were enrolled in this study between September 2004 and November 2005. The patient characteristics are shown in Table 1. Thirty-six of the forty patients showed a KPS of $\geq$90. Prior treatment was gemcitabine monotherapy in all patients. Thirty-six of the forty patients (90%) received gemcitabine as a standard 30 min infusion, and the remaining four patients (10%) received gemcitabine administered by fixed dose rate infusion. Of 40 patients, 4 patients (10%) showed a partial response, 21 patients (53%) showed stable disease, and 12 (30%) patients showed progressive disease in first-line gemcitabine therapy. Three patients had received first-line chemotherapy at another hospital and accurate data about

Table 1 Patient characteristics ($n = 40$)

Age	
Median (range)	62 (36–74)
Gender	
Male	21
Female	19
KPS	
100	17
90	19
80	4
Biliary drainage	
(+)	6
Prior pancreatectomy	
(+)	7
Location of primary tumor	
Head	17
Body	14
Tail	9
Sites of metastasis	
Liver	33
Lymph node	16
Lung	3
Peritoneum	4
Prior chemotherapy	
Gemcitabine[a]	36
FDR-GEM[b]	4
TTP of prior treatment (months)	
Median (range)	2.8 (0.7–13.5)
CEA (ng/ml)	
Median (range)	14.9 (1.1–1,187)
CA19-9 (U/ml)	
Median (range)	4,673 (0.1–2,960,000)

KPS Karnofsky performance status, *TTP* time to progression, *CEA* carcinoembryonic antigen, *CA19-9* carbohydrate antigen 19-9

[a] Gemcitabine as a standard 30-min infusion

[b] FDR-GEM: gemcitabine as a fixed dose rate infusion

treatment response could not be obtained. The median time to progression in the prior treatment was 2.8 months (range 0.7–13.5 months).

Treatments

A total of 94 courses were administered to the 40 patients with a median of two courses per patient (range 1–12). The initial administered dose of S-1 was 80 mg/day in 1 patient, 100 mg/day in 18 patients, and 120 mg/day in 21 patients. Treatment interruption was necessary in 18 patients, due to fatigue (grade 3: one patients, grade 2: one patient, grade 1: two patients), nausea (grade 2: three patients, grade 1: one patient), diarrhea (grade 3: two patients, grade 1: two patients), drainage tube related problem (two patients), grade 3 appetite loss (1), grade 1 leukocytopenia (1), grade 2 hand-foot skin reaction (1), and grade 1 pneumonitis (1). Dose reduction was required in three patients because of grade 3 diarrhea (1), grade 2 fatigue (1), and grade 1 nausea (1). The relative dose intensity was 94.7%. The reasons for discontinuation of treatment were radiologically confirmed progressive disease (PD) in 31 patients, clinical PD without radiological PD in 6 patients, at the patients request due to unacceptable toxicities in 2 patients (grade 2 fatigue and grade 3 anorexia), and loss to follow up in one patient.

Toxicity

All 40 eligible patients were assessable for adverse events. The treatment-related adverse reactions are listed in Table 2. One patient developed grade 3 pneumonitis without neutropenia and required hospitalization, but she recovered from the pneumonitis with antibiotic treatment. As to other grade 3 non-hematological toxicities, aspartate aminotransferase elevation (two patients), alanine aminotransferase elevation (2), fatigue (2), anorexia (2), diarrhea (2) were noted. Regarding hematological toxicities, grade 3 anemia was noted in one patient. No other severe or unexpected adverse reactions were noted. The most common adverse reactions were fatigue (78%) and anorexia (73%), although most of those adverse reactions were tolerable and reversible. Although five patients died within 4 weeks after discontinuation of treatment due to rapid disease progression, no treatment-related deaths were observed.

Efficacy

Out of the total of 40 eligible patients, 38 patients were assessable for response. Two patients discontinued chemotherapy at their request due to unacceptable toxicities (grade 2 fatigue and grade 3 anorexia) and moved to another hospital before tumor assessment. Although no complete response was seen, partial response was obtained in six patients (15, 95%, confidence interval 3.9–26%). Stable disease was noted in 17 patients (43%), and progressive disease in 15 patients (38%). Tumor responses to second-line S-1 therapy are classified according to tumor responses to first-line gemcitabine in Table 3. The serum CA 19-9 level was reduced to less than half in 8 (23%) of 35 patients with a pretreatment serum CA19-9 level of the upper limit of normal or greater. At the time of enrollment, nineteen of forty (47.5%) patients were eligible for the evaluation of clinical benefit response. Out of nineteen evaluable patients, a clinical benefit response was observed in four patients (21%). The median progression free survival time was 2.0 months, and the median survival time was 4.5 months (range 1.2–14.3+) with a 1-year survival rate of 14.1% (Fig. 1).

Table 2 Treatment-related adverse events ($n = 40$): worst grade reported during treatment period

	Grade				Grade 1–4	Grade 3–4
	1	2	3	4	*n* (%)	*n* (%)
Hematological toxicity						
Leukocytes	8	2	0	0	10 (25)	0 (0)
Neutrophils	3	2	0	0	5 (13)	0 (0)
Hemoglobin	5	13	1	0	19 (48)	1 (3)
Platelets	9	0	0	0	9 (23)	0 (0)
Non-hematological toxicity						
Aspartate aminotransferase elevation	13	1	2	0	16 (40)	2 (5)
Alanine aminotransferase elevation	8	1	2	0	11 (28)	2 (5)
Total bilirubin elevation	4	3	0	0	7 (18)	0 (0)
Fatigue	21	8	2	0	31 (78)	2 (5)
Nausea	18	6	0	0	24 (60)	0 (0)
Vomiting	5	1	0	0	6 (15)	0 (0)
Anorexia	22	5	2	0	29 (73)	2 (5)
Stomatitis	11	3	0	0	14 (35)	0 (0)
Diarrhea	8	4	2	0	14 (35)	2 (5)
Rash	3	0	0	0	3 (8)	0 (0)
Pigmentation	6	1	–	–	7 (18)	–
Hand-foot skin reaction	1	1	0	–	2 (5)	0 (0)
Pneumonitis without neutropenia	0	0	1	0	0 (0)	1 (3)

Table 3 Objective tumor response (RECIST criteria) ($n = 40$)

Response (2nd line)	*n* (%)	Response (1st line)			
		PR	SD	PD	NE
CR	0 (0%)	0	0	0	0
PR	6 (15%)	1	4	0	1[a]
SD	17 (43%)	2	9	5	1[a]
PD	15 (38%)	1	6	7	1[a]
NE	2 (5%)	0	2	0	0
Total	40 (100%)	4	21	12	3

Treatment response to second-line S-1 therapy is tabulated according to treatment response to first-line gemcitabine

[a] Three patients received first-line chemotherapy at another hospital and accurate data about treatment ressponse was unobtainable

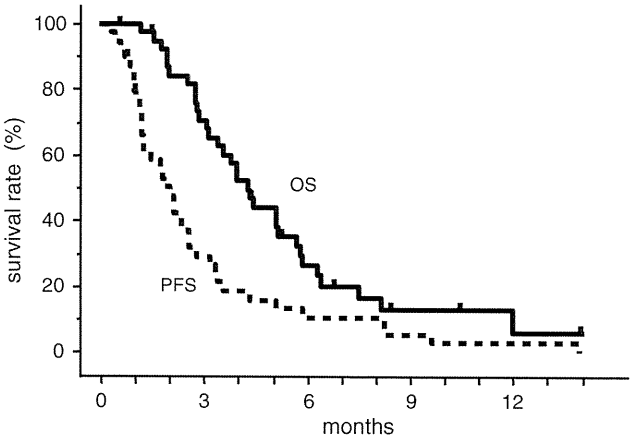

Fig. 1 Survival ($n = 40$). Progression free survival (*dashed line*), and overall survival time (*solid line*) curves of patients with gemcitabine refractory pancreatic cancer receiving systemic chemotherapy with S-1

Discussion

Over the last several years, many studies have been designed to establish effective treatment for gemcitabine-refractory pancreatic cancer patients. So far, the results of two randomized phase III studies had been reported. Jacobs et al. reported on a phase III study comparing Rubitecan, a new topoisomerase I inhibitor, versus "physicians' choice" in 409 pretreated patients. The study was unable to indicate any statistically significant survival benefit in the Rubitecan arm (3.7 months vs. 3.1 months, $P = 0.626$), although progression-free survival was significantly improved in Rubitecan arm (1.9 months vs. 1.6 months, $P = 0.001$) [12]. On the other hand, Oettle et al. [22] reported on phase III study comparing a combination of oxaliplatin, 5-FU and folinic acid with best supportive care (BSC). The BSC arm closed to accrual after 46 out of 165 planned patients were enrolled because physicians deemed it unethical. The median survival of second-line therapy was 21 weeks compared to 10 weeks for the BSC group ($P = 0.0077$). However, a worldwide consensus regarding this result has not been established because of the small number of patients in

this study. Other studies have investigated the feasibility and activity of second-line treatments in phase II studies [1, 4, 7, 17, 19, 26, 27, 33, 36, 38]. Compared with monotherapy, combination regimens exhibited superior activity in these studies. Fluoropyrimidine-, Irinotecan- or oxaliplatin-based combinations indicated relatively preferable activity with objective responses rate of about 20% and a median survival of 5–6 months in this setting [7, 17, 27, 36, 38]. The safety profiles of such combination regimens require further careful evaluation, and well-designed, larger randomized controlled studies are needed.

In the current study, S-1 produced a response rate of 15%, which was superior to the rates obtained for other reported single agents, including paclitaxel (5.5%) [21], raltitrexed (0%) [38], rubitecan (7%) [4]. However, this response rate failed to reach the pre-established boundary of 17.5% required for the agent to be considered effective. Furthermore, the progression-free survival (median 2 months) and the overall survival (median 4.5 months) were still extremely poor in this study. Although S-1 seems to have some degree of anti-tumor activity in patients with gemcitabine refractory metastatic pancreatic cancer, monotherapy may be insufficient to prolong survival. This limitation may be due to the strong chemo-resistance and heterogeneity of the tumors caused by the nature of the disease and acquired from previous chemotherapy regimens.

The toxicity of S-1 was acceptable and no life-threatening toxicities were observed. Although a population with an extremely poor prognosis was targeted in this study and the general condition of the participating patients was expected to be unstable, the toxicities were similar to the results of previous clinical studies for S-1 in chemo-naïve patients with pancreatic cancers [24, 37]. The safety profile of this study suggests that S-1 can be safely administered to pancreatic cancer patients even in a second-line setting, at least in selected populations.

We conclude that S-1 as monotherapy had marginal anti-tumor activity with tolerable toxicity in patients with gemcitabine refractory metastatic pancreatic cancer. In view of the favorable toxicity profile, its combination with other agents might have potential to improve therapeutic results.

References

1. Androulakis N, Syrigos K, Polyzos A, Aravantinos G, Stathopoulos GP, Ziras N, Mallas K, Vamvakas L, Georgoulis V (2005) Oxaliplatin for pretreated patients with advanced or metastatic pancreatic cancer: a multicenter phase II study. Cancer Invest 23:9–12
2. Boeck S, Weigang-Kohler K, Fuchs M, Kettner E, Quietzsch D, Trojan J, Stotzer O, Zeuzem S, Lordick F, Kohne CH, Kroning H, Steinmetz T, Depenbrock H, Heinemann V (2007) Second-line chemotherapy with pemetrexed after gemcitabine failure in patients with advanced pancreatic cancer: a multicenter phase II trial. Ann Oncol 18:745–751
3. Burris HA III, Moore MJ, Andersen J, Green MR, Rothenberg ML, Modiano MR, Cripps MC, Portenoy RK, Storniolo AM, Tarassoff P, Nelson R, Dorr FA, Stephens CD, Von Hoff DD (1997) Improvements in survival and clinical benefit with gemcitabine as first-line therapy for patients with advanced pancreas cancer: a randomized trial. J Clin Oncol 15:2403–2413
4. Burris HA III, Rivkin S, Reynolds R, Harris J, Wax A, Gerstein H, Mettinger KL, Staddon A (2005) Phase II trial of oral rubitecan in previously treated pancreatic cancer patients. Oncologist 10:183–190
5. Cantore M, Rabbi C, Fiorentini G, Oliani C, Zamagni D, Iacono C, Mambrini A, Del Freo A, Manni A (2004) Combined irinotecan and oxaliplatin in patients with advanced pre-treated pancreatic cancer. Oncology 67:93–97
6. Cunningham D, Chau I, Stocken D, Davies C, Dunn J, Valle J, Smith D, Steward W, Harper P, Neoptolemos J (2005) Phase III randomised comparison of gemcitabine (GEM) versus gemcitabine plus capecitabine (GEM-CAP) in patients with advanced pancreatic cancer. ECCO 13—the European Cancer Conference Abstract 717
7. Demols A, Peeters M, Polus M, Marechal R, Gay F, Monsaert E, Hendlisz A, Van Laethem JL (2006) Gemcitabine and oxaliplatin (GEMOX) in gemcitabine refractory advanced pancreatic adenocarcinoma: a phase II study. Br J Cancer 94:481–485
8. Green SJ, Benedetti J, Crowley J (1997) Clinical Trials in Oncology, 1st edn. Chapman & Hall, London
9. Green SJ, Dahlberg S (1992) Planned versus attained design in phase II clinical trials. Stat Med 11:853–862
10. Hryniuk W, Bush H (1984) The importance of dose intensity in chemotherapy of metastatic breast cancer. J Clin Oncol 2:1281–1288
11. Inuyama Y, Kida A, Tsukuda M, Kohno N, Satake B (2001) Late phase II study of S-1 in patients with advanced head and neck cancer. Gan To Kagaku Ryoho 28:1381–1390
12. Jacobs D, Burris HA III, Rivkin S, Ritch PS, Eisenberg PD, Mettinger KL (2004) A randomized phase III study of rubitecan (ORA) vs. best choice (BC) in 409 patients with refractory pancreatic cancer report from a North-American multi-center study. Journal of Clinical Oncology, 2004 ASCO Annual Meeting Proceedings (Post-Meeting Edition). 22, 14S (July 15 Supplement), 4013
13. Kawahara M, Furuse K, Segawa Y, Yoshimori K, Matsui K, Kudoh S, Hasegawa K, Niitani H (2001) Phase II study of S-1, a novel oral fluorouracil, in advanced non-small-cell lung cancer. Br J Cancer 85:939–943
14. Klapdor R, Fenner C (2000) Irinotecan(Campto R): efficacy as third/forth line therapy in advanced pancreatic cancer. Anticancer Res 20:5209–5212
15. Koizumi W, Kurihara M, Nakano S, Hasegawa K (2000) Phase II study of S-1, a novel oral derivative of 5-fluorouracil, in advanced gastric cancer. For the S-1 Cooperative Gastric Cancer Study Group. Oncology 58:191–197
16. Kozuch P, Grossbard ML, Barzdins A, Araneo M, Robin A, Frager D, Homel P, Marino J, DeGregorio P, Bruckner HW (2001) Irinotecan combined with gemcitabine, 5-fluorouracil, leucovorin, and cisplatin (G-FLIP) is an effective and noncrossresistant treatment for chemotherapy refractory metastatic pancreatic cancer. Oncologist 6:488–495
17. Kulke MH, Blaszkowsky LS, Ryan DP, Clark JW, Meyerhardt JA, Zhu AX, Enzinger PC, Kwak EL, Muzikansky A, Lawrence C, Fuchs CS (2007) Capecitabine plus erlotinib in gemcitabine-refractory advanced pancreatic cancer. J Clin Oncol 25:4787–4792
18. Milella M, Gelibter A, Di Cosimo S, Bria E, Ruggeri EM, Carlini P, Malaguti P, Pellicciotta M, Terzoli E, Cognetti F (2004) Pilot study of celecoxib and infusional 5-fluorouracil as second-line

treatment for advanced pancreatic carcinoma. Cancer 101:133–138
19. Mitry E, Ducreux M, Ould-Kaci M, Boige V, Seitz JF, Bugat R, Breau JL, Bouche O, Etienne PL, Tigaud JM, Morvan F, Cvitkovic E, Rougier P (2006) Oxaliplatin combined with 5-FU in second line treatment of advanced pancreatic adenocarcinoma. Results of a phase II trial. Gastroenterol Clin Biol 30:357–363
20. Moore MJ, Goldstein D, Hamm J, Figer A, Hecht JR, Gallinger S, Au HJ, Murawa P, Walde D, Wolff RA, Campos D, Lim R, Ding K, Clark G, Voskoglou-Nomikos T, Ptasynski M, Parulekar W (2007) Erlotinib plus gemcitabine compared with gemcitabine alone in patients with advanced pancreatic cancer: a phase III trial of the National Cancer Institute of Canada Clinical Trials Group. J Clin Oncol 25:1960–1966
21. Oettle H, Arnold D, Esser M, Huhn D, Riess H (2000) Paclitaxel as weekly second-line therapy in patients with advanced pancreatic carcinoma. Anticancer Drugs 11:635–638
22. Oettle H, Pelzer U, Stieler J, Hilbig A, Roll L, Schwaner I, Adler M, Detken S, Dörken B, Riess H (2006) Oxaliplatin/folinic acid/5-fluorouracil [24 h] (OFF) plus best supportive careversus best supportive care alone (BSC) in second-line therapy ofgemcitabine-refractory advanced pancreatic cancer (CONKO 003). ASCO Annual Meeting Proceedings No: 4031
23. Ohtsu A, Baba H, Sakata Y, Mitachi Y, Horikoshi N, Sugimachi K, Taguchi T (2000) Phase II study of S-1, a novel oral fluorophyrimidine derivative, in patients with metastatic colorectal carcinoma. S-1 Cooperative Colorectal Carcinoma Study Group. Br J Cancer 83:141–145
24. Okusaka T, Funakoshi A, Furuse J, Boku N, Yamao K, Ohkawa S, Saito H (2007) A late phase II study of S-1 for metastatic pancreatic cancer. Cancer Chemother Pharmacol
25. Reni M, Cordio S, Milandri C, Passoni P, Bonetto E, Oliani C, Luppi G, Nicoletti R, Galli L, Bordonaro R, Passardi A, Zerbi A, Balzano G, Aldrighetti L, Staudacher C, Villa E, Di Carlo V (2005) Gemcitabine versus cisplatin, epirubicin, fluorouracil, and gemcitabine in advanced pancreatic cancer: a randomised controlled multicentre phase III trial. Lancet Oncol 6:369–376
26. Reni M, Panucci MG, Passoni P, Bonetto E, Nicoletti R, Ronzoni M, Zerbi A, Staudacher C, Di Carlo V, Villa E (2004) Salvage chemotherapy with mitomycin, docetaxel, and irinotecan (MDI regimen) in metastatic pancreatic adenocarcinoma: a phase I and II trial. Cancer Invest 22:688–696
27. Reni M, Pasetto L, Aprile G, Cordio S, Bonetto E, Dell'Oro S, Passoni P, Piemonti L, Fugazza C, Luppi G, Milandri C, Nicoletti R, Zerbi A, Balzano G, Di Carlo V, Brandes AA (2006) Raltitrexed-eloxatin salvage chemotherapy in gemcitabine-resistant metastatic pancreatic cancer. Br J Cancer 94:785–791
28. Rothenberg ML, Moore MJ, Cripps MC, Andersen JS, Portenoy RK, Burris HA III, Green MR, Tarassoff PG, Brown TD, Casper ES, Storniolo AM, Von Hoff DD (1996) A phase II trial of gemcitabine in patients with 5-FU-refractory pancreas cancer. Ann Oncol 7:347–353
29. Saek T, Takashima S, Sano M, Horikoshi N, Miura S, Shimizu S, Morimoto K, Kimura M, Aoyama H, Ota J, Noguchi S, Taguchi T (2004) A phase II study of S-1 in patients with metastatic breast cancer—a Japanese trial by the S-1 Cooperative Study Group, Breast Cancer Working Group. Breast Cancer 11:194–202
30. Sakata Y, Ohtsu A, Horikoshi N, Sugimachi K, Mitachi Y, Taguchi T (1998) Late phase II study of novel oral fluoropyrimidine anticancer drug S-1 (1 M tegafur-0.4 M gimestat-1 M otastat potassium) in advanced gastric cancer patients. Eur J Cancer 34:1715–1720
31. Shirasaka T, Shimamato Y, Ohshimo H, Yamaguchi M, Kato T, Yonekura K, Fukushima M (1996) Development of a novel form of an oral 5-fluorouracil derivative (S-1) directed to the potentiation of the tumor selective cytotoxicity of 5-fluorouracil by two biochemical modulators. Anticancer Drugs 7:548–557
32. Shirasaka T, Shimamoto Y, Fukushima M (1993) Inhibition by oxonic acid of gastrointestinal toxicity of 5-fluorouracil without loss of its antitumor activity in rats. Cancer Res 53:4004–4009
33. Stathopoulos GP, Boulikas T, Vougiouka M, Rigatos SK, Stathopoulos JG (2006) Liposomal cisplatin combined with gemcitabine in pretreated advanced pancreatic cancer patients: a phase I–II study. Oncol Rep 15:1201–1204
34. Stehlin JS, Giovanella BC, Natelson EA, De Ipolyi PD, Coil D, Davis B, Wolk D, Wallace P, Trojacek A (1999) A study of 9-nitrocamptothecin (RFS-2000) in patients with advanced pancreatic cancer. Int J Oncol 14:821–831
35. Tatsumi K, Fukushima M, Shirasaka T, Fujii S (1987) Inhibitory effects of pyrimidine, barbituric acid and pyridine derivatives on 5-fluorouracil degradation in rat liver extracts. Jpn J Cancer Res 78:748–755
36. Tsavaris N, Kosmas C, Skopelitis H, Gouveris P, Kopterides P, Loukeris D, Sigala F, Zorbala-Sypsa A, Felekouras E, Papalambros E (2005) Second-line treatment with oxaliplatin, leucovorin and 5-fluorouracil in gemcitabine-pretreated advanced pancreatic cancer: a phase II study. Invest New Drugs 23:369–375
37. Ueno H, Okusaka T, Ikeda M, Takezako Y, Morizane C (2005) An early phase II study of S-1 in patients with metastatic pancreatic cancer. Oncology 68:171–178
38. Ulrich-Pur H, Raderer M, Verena Kornek G, Schull B, Schmid K, Haider K, Kwasny W, Depisch D, Schneeweiss B, Lang F, Scheithauer W (2003) Irinotecan plus raltitrexed vs raltitrexed alone in patients with gemcitabine-pretreated advanced pancreatic adenocarcinoma. Br J Cancer 88:1180–1184

Plasma L-Cystine/L-Glutamate Imbalance Increases Tumor Necrosis Factor-Alpha from CD14+ Circulating Monocytes in Patients with Advanced Cirrhosis

Eiji Kakazu[1], Yoshiyuki Ueno[1]*, Yasuteru Kondo[1], Jun Inoue[1], Masashi Ninomiya[1], Osamu Kimura[1], Yuta Wakui[1], Koji Fukushima[1], Keiichi Tamai[2], Tooru Shimosegawa[1]

1 Division of Gastroenterology, Tohoku University Graduate School of Medicine, Aobaku, Sendai, Japan, **2** Miyagi Cancer Center, Natori, Japan

Abstract

Background and Aims: The innate immune cells can not normally respond to the pathogen in patients with decompensated cirrhosis. Previous studies reported that antigen-presenting cells take up L-Cystine (L-Cys) and secrete substantial amounts of L-Glutamate (L-Glu) via the transport system Xc- (4F2hc+xCT), and that this exchange influences the immune responses. The aim of this study is to investigate the influence of the plasma L-Cys/L-Glu imbalance observed in patients with advanced cirrhosis on the function of circulating monocytes.

Methods: We used a serum-free culture medium consistent with the average concentrations of plasma amino acids from patients with advanced cirrhosis (ACM), and examined the function of CD14+ monocytes or THP-1 under ACM that contained 0–300 nmol/mL L-Cys with LPS. In patients with advanced cirrhosis, we actually determined the TNF-alpha and xCT mRNA of monocytes, and evaluated the correlation between the plasma L-Cys/L-Glu ratio and TNF-alpha.

Results: The addition of L-Cys significantly increased the production of TNF alpha from monocytes under ACM. Monocytes with LPS and THP-1 expressed xCT and a high level of extracellular L-Cys enhanced L-Cys/L-Glu antiport, and the intracellular GSH/GSSG ratio was decreased. The L-Cys transport was inhibited by excess L-Glu. In patients with advanced cirrhosis (n = 19), the TNF-alpha and xCT mRNA of monocytes were increased according to the Child-Pugh grade. The TNF-alpha mRNA of monocytes was significantly higher in the high L-Cys/L-Glu ratio group than in the low ratio group, and the plasma TNF-alpha was significantly correlated with the L-Cys/L-Glu ratio.

Conclusions: A plasma L-Cys/L-Glu imbalance, which appears in patients with advanced cirrhosis, increased the TNF-alpha from circulating monocytes via increasing the intracellular oxidative stress. These results may reflect the immune abnormality that appears in patients with decompensated cirrhosis.

Citation: Kakazu E, Ueno Y, Kondo Y, Inoue J, Ninomiya M, et al. (2011) Plasma L-Cystine/L-Glutamate Imbalance Increases Tumor Necrosis Factor-Alpha from CD14+ Circulating Monocytes in Patients with Advanced Cirrhosis. PLoS ONE 6(8): e23402. doi:10.1371/journal.pone.0023402

Editor: Stefan Bereswill, Charité-University Medicine Berlin, Germany

Received June 27, 2011; **Accepted** July 15, 2011; **Published** August 17, 2011

Copyright: © 2011 Kakazu et al. This is an open-access article distributed under the terms of the Creative Commons Attribution License, which permits unrestricted use, distribution, and reproduction in any medium, provided the original author and source are credited.

Funding: This study was supported in part by a grant-in-aid from the Ministry of Education, Culture, Sports, Science, and Technology of Japan to EK (23790762), and by Health and Labour Sciences Research Grants for the Research on Measures for Intractable Diseases (from the Ministry of Health, Labour and Welfare of Japan) to YU. The funders had no role in study design, data collection and analysis, decision to publish, or preparation of the manuscript.

Competing Interests: The authors have declared that no competing interests exist.

* E-mail: yueno@med.tohoku.ac.jp

Introduction

Circulating levels of proinflammatory cytokines such as TNF-alpha, IL-1 beta and IL-6 are increased in patients with cirrhosis [1,2,3]. Endotoxemia has been assumed to be responsible for the increased of such cytokines in patients with cirrhosis [4], because the activation of monocytes, macrophages and dendritc cells (DCs) by lipopolysaccharide (LPS) plays a key role in the pathogenesis of cytokine overproduction. This overproduction of proinflammatory cytokines leads to various complications, such as spontaneous bacterial peritonitis (SBP) and hepatorenal syndrome (HRS) in patients with advanced cirrhosis [5,6].

On the other hand, various types of amino acid imbalance appear in the plasma of patients with decompensated cirrhosis, since the liver plays a major role in metabolism involving glucose, lipids, vitamins,minerals and amino acids. An imbalance of plasma amino acids, with decreased levels of branched-chain amino acids (BCAAs) and increased levels of aromatic amino acids (AAAs), is commonly seen in patients with advanced cirrhosis [7]. Previously, we reported that extracellular branched-chain amino acids (BCAAs) regulate the maturation and function of monocyte derived dendritic cells [8], and that the addition of branched chain amino acids enhances the maturation and function of myeloid dendritic cells ex vivo in patients with advanced cirrhosis [9]. However, it is not clear whether the imbalance of amino acids other than BCAAs influence the immune responses in patients with advanced cirrhosis. A previous study showed that the concentration of plasma L- Cystine (L-Cys) is higher in patients with cirrhosis and shows a wide range of variation [10]. Increased levels of L-Glutamine (L-Gln) and decreasing levels of

L-Glutamate (L-Glu) are seen in patients with advanced cirrhosis, because the L-Glu-L-Gln exchange regulates the high levels of toxic ammonia in such patients [11]. Furthermore, previous studies demonstrated that antigen-presenting cells take up L-Cys via the Na-independent anionic amino acid transport system Xc^-(4F2hc+xCT) and secrete substantial amounts of L-Glu, influencing the immune-responses through this exchange [12,13,14]. This transporter is composed of two protein components, xCT and 4F2hc (CD98), and the transport activity is thought to be mediated by xCT [15,16]. The aim of this study is to investigate the influence of the extracellular L-Cys/L-Glu imbalance observed in patients with advanced cirrhosis on the function of peripheral monocytes using a serum-free culture medium with the average concentration of plasma amino acids from patients with advanced cirrhosis [9], thereby approximating the actual environment of the living body.

Materials and Methods

Ethics Statement

Written informed consent was obtained from each individual and the study protocol was approved by the Ethics Committee of Tohoku University School of Medicine (2009-209, 2009-535).

Monocyte count and isolation

In patients with cirrhosis, the monocyte and lymphocyte counts were measured by a Beckman Coulter LH 750 Analyzer (Fullerton, CA, USA). PBMCs were separated from the peripheral blood of healthy volunteers or patients with cirrhosis by centrifugation on a density gradient. The CD14-positive monocytes were isolated from PBMCs using magnetic microbeads (Miltenyi Biotec, Bergish Gladbach).

The serum free culture media used in this study

A serum free culture medium with the average concentration of plasma amino acids from healthy volunteers (HCM), that from patients with advanced cirrhosis (ACM) and complete culture media (CCM) were described previously [9]. Other components except amino acids were identical among media. Various concentrations of L-Cys were added to L-Cys free ACM , and the final concentration was adjusted to 0–300 nmol/mL (Table S1). We cultured CD14+monocytes, THP-1, Jurkat and Molt-4 under the these media with stimulant and measured the amino acid concentrations of these media. The viability of monocytes and PBMCs was determined using Annexin V^{FITC}, with dead cells identified by propidium iodide (PI) staining (Annexin V^{-FITC} Apoptosis Detection Kit, BioVision, Mountain View, CA), according to the manufacturer's instructions. We confirmed the viability of PBMCs cultured in ACM and ACM plus L-Cys to be equal to that of complete culture medium (CCM) and X-VIVO 10 (Cambrex Bio Science Walkersville, Inc. Walkersville, MD USA).

Patients and Healthy volunteers

The concentrations of the plasma amino acids from fasting patients with chronic hepatitis (n = 17), and patients with cirrhosis (n = 130) were measured by high-performance liquid

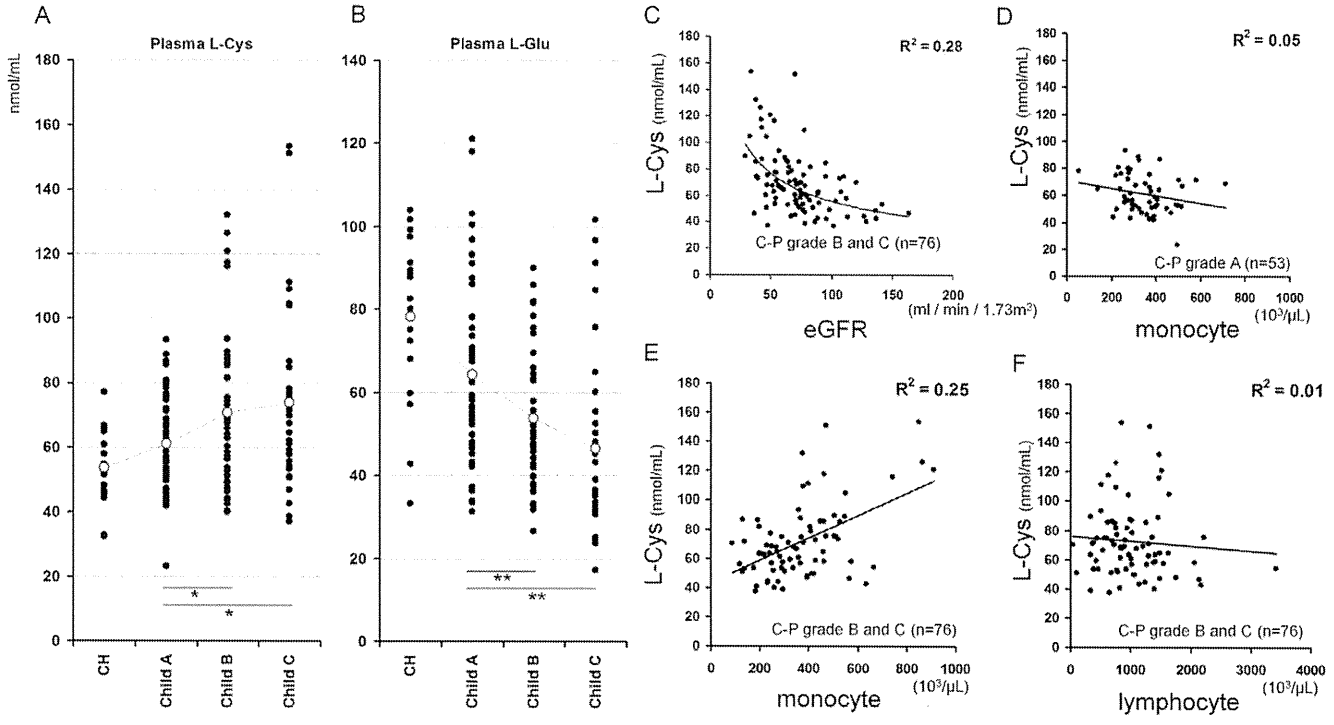

Figure 1. The counts of peripheral monocyte were increased in association with plasma L-Cystine in patients with advanced cirrhosis. A, B, The concentrations of plasma L-Cys in patients with cirrhosis was increased and that of plasma L-Glu was decreased acccording to Child-Pugh grade. The levels of plasma L-Cys and L-Glu in patients with cirrrhosis (n = 130) were measured using HPLC and classfied by the Child-Pugh classfication. C, Nonliner regression model was used to model variation in plasma L-Cys and eGFR. D, E,F, Linear regression model was used to model variation in plasma L-Cys and monocyte and lymphocyte counts. Individual correlations between plasma L-Cys levels and monocyte counts in patients with early cirrhosis (D), that in patients with advanced cirrhosis (E), and lymphocyte counts in patients with advanced cirrhosis (F). A,B, **, $p<0.01$, _*, $p<0.05$ vs Child-Pugh grade A. Statistical significance was determined by one-way ANOVA and Dunnett's post-hoc procedure. C, D, E, F, R^2 represents coefficient of determination.
doi:10.1371/journal.pone.0023402.g001

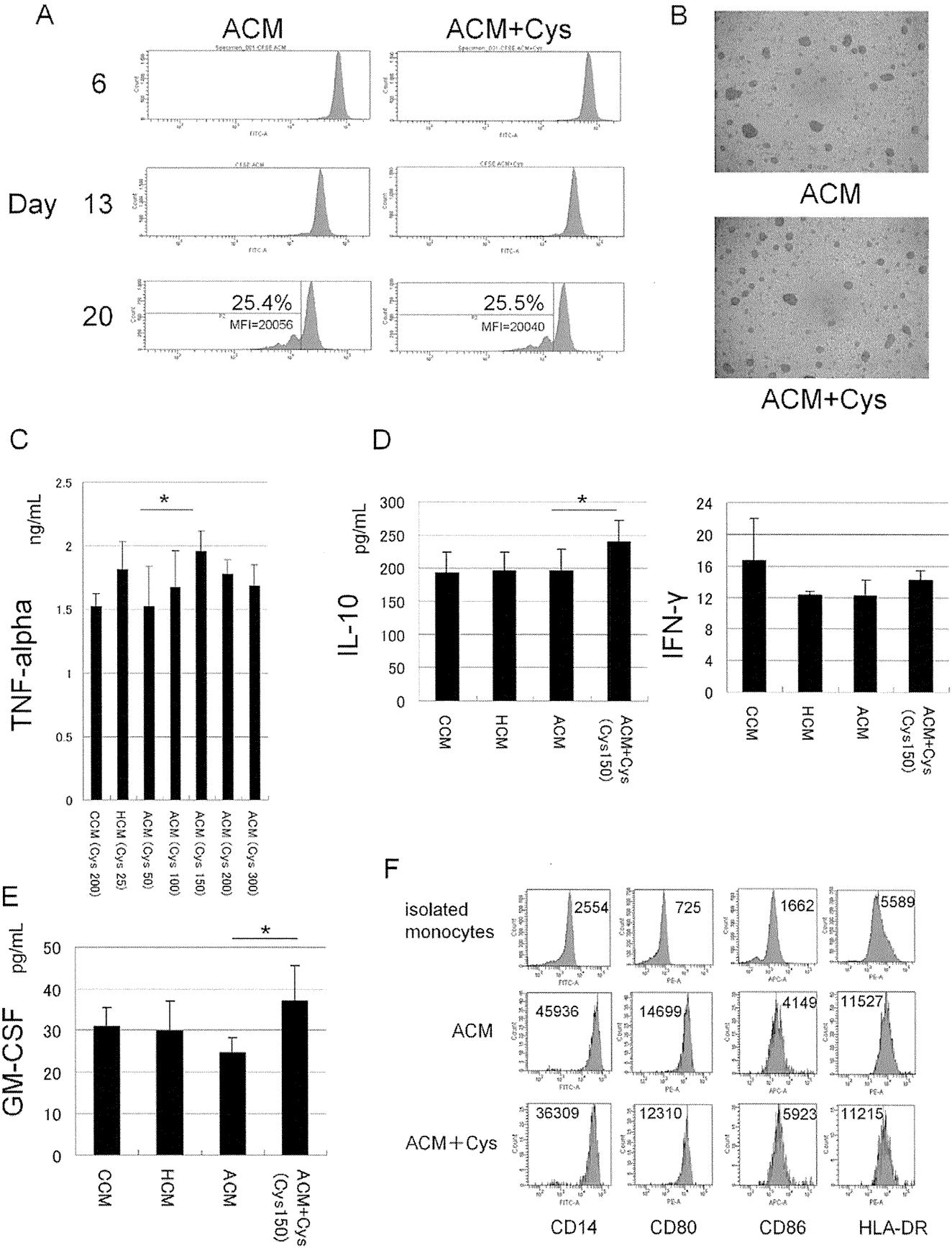
A
ACM
ACM+Cys
6
Day 13
20
25.4%
MFI=20056
25.5%
MFI=20040
B
ACM
ACM+Cys
C
TNF-alpha
ng/mL
2.5
2
1.5
1
0.5
0
*
CCM (Cys 200)
HCM (Cys 25)
ACM (Cys 50)
ACM (Cys 100)
ACM (Cys 150)
ACM (Cys 200)
ACM (Cys 300)
D
IL-10
pg/mL
300
250
200
150
100
50
0
*
CCM
HCM
ACM
ACM+Cys (Cys150)
IFN-γ
24
20
16
12
8
4
0
CCM
HCM
ACM
ACM+Cys (Cys150)
E
GM-CSF
pg/mL
50
40
30
20
10
0
*
CCM
HCM
ACM
ACM+Cys (Cys150)
F
isolated monocytes
ACM
ACM+Cys
2554
725
1662
5589
45936
14699
4149
11527
36309
12310
5923
11215
CD14
CD80
CD86
HLA-DR

Figure 2. L-Cystine dose-dependently increased TNF-alpha from CD14+ monocytes with LPS under the amino acid environment of patients with advanced cirrhosis. A, Isolated CD14+ monocytes (purity >90%) were cultured at a density of 2.5×10^5 cells/well in 96-well plates containing in ACM and ACM plus L-Cys (L-Cys : 150 nmol/mL) with 1,000 U/mL M-CSF. One half the amount of culture fluid was exchanged every one day. Cells were maintained for 20 days and the proliferation rate of the cells was measured using CFSE staining. B, Influence of L-Cys on microscopic appearance of monocyte proliferation under serum-free conditions. Day 20, cells in firmly adherent clusters in both ACM and ACM+Cys. C, Monocytes were cultured under CCM, HCM, ACM and ACM plus L-Cys (100–300 nmol/mL). Cells were pre-incubated at a density of 2.5×10^5 cells/well in 96-well flat-bottom plates for 2 hours in each of the media, and 100 ng/mL LPS was added. The supernatants were collected after 24 hours and immediately TNF-alpha was determined by specific cytokine ELISA kits. D,E, Similarly as in Fig. 2C, IL-10, IFN gamma from monocytes and GM-CSF from PBMCs under CCM, HCM, ACM, ACM+Cys (L-Cys 150 nmol/mL) were measured with ELISA. F, Cells were harvested after 24 hours, stained with different mAbs, and analyzed using flow cytometry. Cells were stained with FITC-labeled anti-CD14, -CD80, -CD86, and -HLA-DR. A, B and F results are representative of four experiments from three different donors. C, D and E, Mean ± SEM values from five different donors are shown. C,D,E *, $p<0.05$ vs ACM (paired Student's t test, two-tailed).
doi:10.1371/journal.pone.0023402.g002

chromatography (HPLC) in the early morning. Briefly, sulfosalicylic acid was added to the plasma to a final concentration of 5%. The samples were then placed on ice for 15 minutes followed by centrifugation to remove precipitated proteins. The extracts were then analyzed for the amino acid content with a JLC-500/V (Japan Electron Optics Laboratories, Tokyo, Japan). Also, the patients with cirrhosis were classified according to the Child-Pugh classification. We defined as Child-Pugh grade B or C the patients with advanced cirrhosis. The estimated glomerular filtration rate (eGFR) was calculated using the new Japanese equation [17].

We selected nineteen patients with cirrhosis for in vitro or ex vivo studies (Table S2). All of these patients were inpatients. The MELD score [18] was calculated by an on-line worksheet available on the internet at www.mayoclinic.org/meld/mayomodel5.html.

Monocyte proliferation assay

Monocytes were cultured at a density of 2.5×10^5 cells/well in 96-well plates containing each media with 1,000 U/mL M-CSF (PEPROTECH EC, London, UK). One half the amount of culture fluid was exchanged every one day. Cells were maintained for 20 days and the proliferation rate of the cells was measured using Carboxyfluorescein Succinimidyl Ester (CFSE) staining; CellTrace CFSE Cell Proliferation Kit (Molecular Probes, Oregon). The staining methods followed the manufacturer's protocol.

Cytokine analysis

PBMCs or monocytes were preincubated at a density of 2.5×10^5 cells/well in 96-well flat-bottom plates (CORNING, NY) for 2 hours in each of the media, and 100 ng/mL LPS (Escherichia coli 026:B6 (SIGMA) were added. The supernatants were collected after 24 hours and immediately TNF-alpha, IFN-gamma, IL-10, GM-CSF were determined by specific cytokine ELISA kits (Bender MedSystems) according to the manufacturer's instructions.

Surface marker analysis

Monocytes were harvested and labeled with FITC-, PE- and APC-labeled monoclonal antibodies (mAbs) (anti-human CD14, CD80, CD86, CD98, HLA-DR, or the relevant isotype controls: BD PharMingen, San Diego, CA), according to the manufacturer's instructions. On xCT expression, indirect staining was performed; primary antibody (xCT (H-121) scc-98552: Santa Cruz) secondary antibody (goat anti-rabbit IgG-FITC sc-2012: Santa Cruz) Using a FACS Canto II (BD Immunocytometry Systems, San Diego, CA) flow cytometer, surface marker expressions were analyzed using the BD FACSDiva (BD Immunocytometry Systems) program.

Intra-extracellular amino acid quantification

The THP-1, Jurkat and Molt4 cells were pre-incubated for 2 hr in ACM, then 1.0×10^7 cells were re-suspended with LPS (100 ng/mL) or IL-2 (1000 IU/mL) in 1 mL of ACM, L-Cys-free ACM or ACM with L-Cys. After 2 hr incubation, the supernatants were measured by HPLC for the extracellular amino acid quantification. The concentration of the intracellular amino acids was determined as described in ref [19]. Briefly, cells were washed two times by PBS and resuspended in 500 µL PBS sonicated with four 10-s pulses. Cell debris was removed by centrifugation, and sulfosalicylic acid was added to the supernatant to a final concentration of 2%. The samples were then placed on ice for 30 min followed by centrifugation to remove precipitated proteins. The extracts were then analyzed for amino acid content with an L-8500 amino acid analyzer (Hitachi Ltd., Tokyo).

Measurement of reduced glutathione (GSH) and oxidized glutathione (GSSG)

CD14+ monocytes were pre incubated at a density of 2.0×10^5 cells/well in 96-well plates containing HCM for 2 h and then cultured in HCM, ACM or ACM plus L-Cys for an additional 2 h. The culture medium was carefully removed from the wells. 100 µl of prepared GSH-Glo™ Reagent were added to each well of a 96-well plate, mixed briefly on a plate shaker, and incubated at room temperature for 30 minutes. 100 µl of reconstituted Luciferin Detection Reagent were added to each well of a 96-well plate, mixed briefly on a plate shaker, and incubated for 15 minutes. luminescence was read by a Lumino Skan Ascent (Thermo BioAnalysis, Helsinki, Finland).

Real-time PCR

THP-1, Jurkat, Molt-4 and CD14+ monocytes were collected. After the extraction of total RNA and the RT procedure, real-time PCR using aTaqMan Chemistry System () was carried out. The ready-made sets of primers and probes for the amplification of xCT (Assay ID : Hs00921937_m1), TNF-alpha (Assay ID : Hs99999043_m1) and glyceraldehyde-3-phosphate-dehydrogenase (GAPDH, Assay ID : Hs02758991_g1) were purchased from Perkin-Elmer/Applied Biosystems. The relative amount of target mRNA was obtained by using a comparative threshold cycle (CT) method. The expression level of mRNAs of the Molt-4 was represented as 1.0 and the relative amounts of target mRNA in THP-1 and Jurkat were calculated according to the manufacturer's protocol. For CD14+ monocytes, The expression level of monocyte mRNA from a healthy volunteer was represented as 1.0 and the relative amounts of target mRNA in monocytes from patients were calculated.

Statistical Analysis

The data were analyzed with ANOVA, and multiple comparisons were performed with Dunnett's post-hoc procedure for the plasma aminogram. When 2 groups were analyzed, the differences between media were analyzed by the Wilcoxon t test, and the

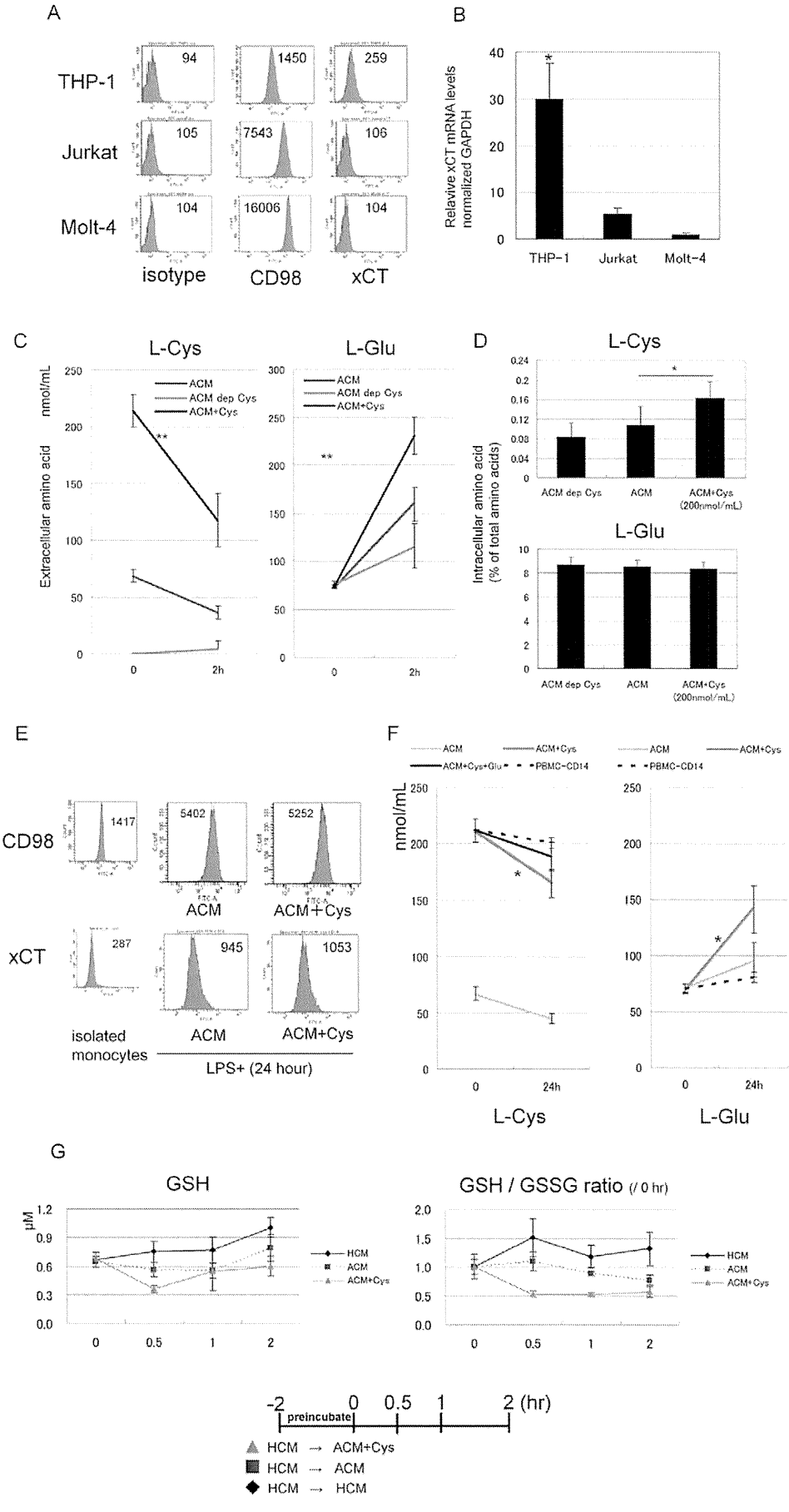
A
THP-1
Jurkat
Molt-4
94
1450
259
105
7543
106
104
16006
104
isotype
CD98
xCT
B
Relavive xCT mRNA levels normalized GAPDH
THP-1
Jurkat
Molt-4
C
L-Cys
L-Glu
nmol/mL
Extracellular amino acid
ACM
ACM dep Cys
ACM+Cys
D
L-Cys
L-Glu
Intracellular amino acid (% of total amino acids)
ACM dep Cys
ACM
ACM+Cys (200nmol/mL)
E
CD98
xCT
1417
5402
5252
287
945
1053
ACM
ACM+Cys
isolated monocytes
LPS+ (24 hour)
F
ACM
ACM+Cys
ACM+Cys+Glu
PBMC-CD14
nmol/mL
L-Cys
L-Glu
G
GSH
GSH / GSSG ratio (/ 0 hr)
μM
HCM
ACM
ACM+Cys
-2
0
0.5
1
2 (hr)
preincubate
HCM → ACM+Cys
HCM → ACM
HCM → HCM

Figure 3. High levels of extracellular L-Cystine promoted the L-Cystine-L-Glutamate antiport via xCT and decreased the intracellular GSH/GSSG ratio in monocyte under the amino acid environment of patients with advanced cirrhosis. A, THP-1, Jurkat and Molt-4 cultured under CCM were harvested and labeled with antibodies (CD98, xCT or the relevant isotype controls). Using flow cytometry, surface marker expressions were analyzed. The figure expresses the mean fluorescence intensity. Data shown are representative of three independent experiments with cells. B, xCT relative mRNA levels of these cell lines were determined by real time PCR: delta-delta CT method. All mRNA expression levels were normalized to GAPDH. C, D, The THP-1 cells were pre-incubated for 2 hours in ACM, then resusupended with LPS (100 ng/mL) in 1 mL of ACM, L-Cys-free ACM and ACM plus L-Cys. The concentration of extracellular (C) and intracellular (D) amino acid was determined as described in material and methods. E, The CD14+ monocytes, cultured under ACM and ACM plus L-Cys for 24 hours, were harvested and labeled with antibodies (CD98, xCT or the relevant isotype controls). Using flow cytometry, surface marker expressions were analyzed. The figure expresses the mean fluorescence Intensity. Data shown are representative of three independent experiments with cells. F, Similarly as in Fig. 4C, the monocytes were cultured for 24 hours in ACM, L-Cys-free ACM and ACM plus L-Cys. The supernatants were measured by HPLC as extracellular amino acids quantification. G, Monocytes were pre incubated at a density of 2.0×10^5 cells/well in 96-well flat-bottom plates for 2 hours in HCM, and then cultured in HCM, ACM and ACM plus L-Cys (200 nmol/mL) for an additional 2 hours. These intracellular glutathione levels were measured by GSH-Glo™ at the time point indicated. C and D, Mean ± SD values from five independent experiments are shown. B *, $p<0.05$ vs Molt-4 (the Mann-Whitney U-test.). C,F **, $p<0.01$ *,$P<0.05$ (mean change vs ACM) D *, $p<0.05$ (paired Student's t test, two-tailed).
doi:10.1371/journal.pone.0023402.g003

differences between healthy controls and patients were analyzed by the Mann-Whitney U-test. All statistical analyses were performed with standard statistical software (SPSS 13.0 for Windows, Chicago, IL).

Results

The counts of peripheral monocytes were increased in association with the plasma L-Cystine in patients with advanced cirrhosis

Firstly, we confirmed that, in patients with advanced cirrhosis (Child-Pugh grade B or C), the plasma concentrations of L-Cys were significantly higher than in those with early cirrhosis (Figure 1A), and there was a wide range of variation. On the other hand, the plasma concentrations of L-Glu were significantly decreased along with the Child-Pugh grade (Figure 1B). In patients with advanced cirrhosis, the wide range of variation of L-Cys was attributed to the eGFR ($R^2=0.28/P=0.0000008$) (Figure 1C). These data mean that plasma L-Cys increases in decompensated cirrhosis. Secondly, we investigate whether the concentration of plasma L-Cys influenced the peripheral monocyte counts. In patients with early cirrhosis, L-Cys was not correlated with the monocyte counts ($R^2=0.05/P=0.119$) (Figure 1D), but in patients with advanced cirrhosis, it was significantly and positively correlated with the monocyte counts ($R^2=0.25/P=0.0000017$) (Figure 1E). On the other hand, the lymphocyte counts were not correlated with the concentration of plasma L-Cys ($R^2=0.01/P=0.523$) (Figure 1F). Interestingly, among all twenty kinds of free amino acids, only L-Cys was significantly correlated with the monocyte counts in patients with advanced cirrhosis (Figure S1). These data mean that, in patients with advanced cirrhosis, plasma L-Cys is increased according to renal dysfunction and influences the counts of monocytes.

Extracellular L-Cystine dose-dependently increased pro-inflammatory cytokines from CD14+ monocytes under the amino acid condition of advanced cirrhosis

Based on the result that the peripheral monocyte counts were positively correlated with the concentration of L-Cys, we hypothesized that the concentration of extracellular L-Cys could influence the proliferation of monocytes. To investigate this hypothesis, we cultured monocytes for 20 days with M-CSF under ACM or ACM plus L-Cys in vitro, and determined the proliferation of monocytes by CFSE assay. An elevated concentration of L-Cys did not influence the proliferation of monocytes (Figure 2A) on microscopic appearance, and also did not affect the morphological appearance and behavior of the cells in culture (Figure 2B). There was also no difference in the proliferation of the monocyte cell line, THP-1 between these media (data not shown). Next, to investigate whether the extracellular L-Cys level influenced the production of inflammatory cytokines from monocytes, we cultured monocytes under ACM that contained 50–300 nmol/mL L-Cys and measured the producton of TNF alpha from monocytes. The addition of L-Cys increased the production of TNF alpha from monocytes in a dose-dependent manner (Figure 2C), and the values were maximum under 150 nmol/mL L-Cys. Interestingly, this range was in remarkable agreement with the range in patients with advanced cirrhosis (Fig. 1A). The IL-10 level from monocytes was also significantly higher under ACM plus L-Cys than that under ACM (Figure 2D), and there was no difference the interferon gamma (IFN γ) level from monocytes between these media. The GM-CSF from PBMCs was also significantly higher under ACM plus L-Cys than that under ACM (Figure 2E). Regarding monocyte phenotypes, there was no difference between ACM and ACM plus L-Cys (Figure 2F). These data mean that high levels of extracellular L-Cys increased pro-inflammatory cytokines from CD14+ monocytes under the amino acid environment of patients with advanced cirrhosis.

High levels of extracellular L-Cystine promoted the L-Cystine-L-Glutamate antiport and decreased the intracellular GSH/GSSG ratio in monocyte under the amino acid environment of patients with advanced cirrhosis

We investigated whether high levels of extracellular L-Cys influence the L-Cys/L-Glu transport under the amino acid environment of patients with advanced cirrhosis.

Firstly, we determined the expression of 4F2hc (CD98) and xCT in THP-1, Jurkat and Molt-4. All cell lines expressed CD98, but only THP-1 expressed xCT at the protein level (Fig. 3A) and mRNA level (Fig. 3B). Secondly, we measured the intra-extracellular L-Cys and L-Glu concentration of THP-1 under ACM at various L-Cys levels. After 2 hours culture, ACM plus L-Cys significantly decreased the extracellular L-Cys (mean change, ACM+Cys, −96.8±15.8; ACM, −32.3±0.6 and ACM dep L-Cys, 4.8±6.6 nmol/mL) (Fig. 3C) and significantly increased intracellular L-Cys (Fig. 3D) and extracellular L-Glu (mean change, ACM+Cys, 157.5±19; ACM, 86.1±17.7 and ACM dep L-Cys, 40.4±24.9 nmol/mL) (Fig. 3C) more than that by ACM or ACM deprived of L-Cys. For intracellular L-Glu, there was no difference among these media. Such L-Cys/L-Glu changes were not seen for Jurkat and Molt-4 (data not shown). These data indicate that high levels of extracellular L-Cys enhances L-Cys/L-Glu antiport in the monocyte cell line THP-1. Similarly, CD14+ monocytes expressed CD98 and xCT after adding LPS (Fig. 3E) and extracellular L-Cys/L-Glu changes were seen (L-Cys mean change, ACM+Cys, −46.9±5.0; ACM, −22.4±6.0; ACM+Cys+Glu, −22.9±6.4 and

PBMC-CD14, −11.0±11.9 nmol/mL/L-Glu mean change; ACM+Cys, 70.4±24.8; ACM, 25.2±13.8 and PBMC-CD14, 10.7±7.0 nmol/mL) (Fig. 3F). Furthermore, we investigated whether high levels of extracellular L-Cys influence the intracellular glutathione level of monocytes. Interestingly, the intracellular GSH and GSH/GSSG ratio decreased more under ACM plus L-Cys than under ACM or HCM (Fig. 3G).

Plasma L-Cys/L-Glu ratio significantly correlated with plasma TNF-alpha level in patients with advanced cirrhosis

Finally, we actually measured the levels of TNF-alpha of patients with advanced cirrhosis in monocytes and plasma (Table S2). In patients with advanced cirrhosis (Table S2: patients 1–19), the TNF-alpha mRNA expression of monocytes was significantly

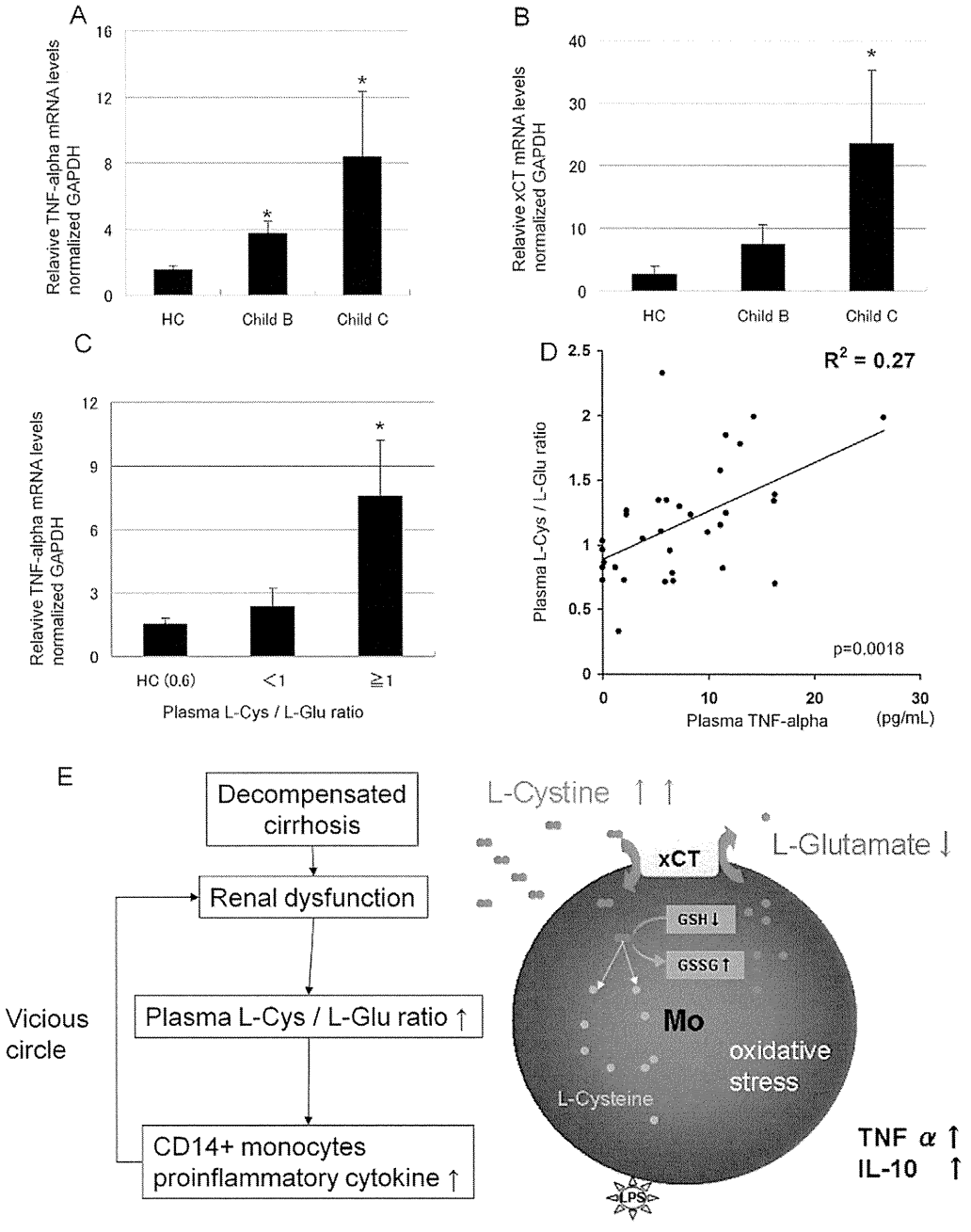

Figure 4. The plasma L-Cys/L-Glu ratio significantly correlated with the plasma TNF-alpha level in patients with advanced cirrhosis. A, CD14+monocytes were isolated from healthy volunteers (n = 5) and patients with adcanced cirrhosis (Table S2 : Patient 1–19). the TNF-alpha relative mRNA levels of CD14+monocytes were determined by real time PCR : delta-delta CT method. All mRNA expression levels were normalized to GAPDH. B, Similarly as in Fig. 4A, the xCT relative mRNA levels of monocytes were determined by real time PCR. C, These patients were separated into a high L-Cys/L-Glu ratio group (≥1) and low ratio group (<1). In healthy control (HC), the average plasma L-Cys/L-Glu ratio was 0.61±0.21. D, Linear regression model was used to model variation in plasma L-Cys/L-Glu ratio and plasma TNF-alpha. R^2 represents coefficient of determination. E, The schematic diagram of the present study concerning monocytes abnormality in patients with decompensated cirrhosis. A,B,C *, $p<0.05$ vs HC (the Mann-Whitney U-test.).

doi:10.1371/journal.pone.0023402.g004

higher than that of healthy controls (Fig. 4A), and xCT mRNA expressions also was increased according to the Child-pugh grade (Fig. 4B). Interestingly, the TNF-alpha mRNA of monocytes was significantly higher in the high plasma L-Cys/L-Glu ratio group (≥ 1) than in the low group (<1) (Fig. 4C). Consistent with these data, the plasma TNF-alpha in the patients was significantly correlated with the plasma L-Cys/L-Glu ratio ($p = 0.0018/r = 0.52247$) (Fig. 4D). We represented the schematic diagram of the present study concerning monocytes abnormality in patients with decompensated cirrhosis (Fig. 4E).

Discussion

Bacterial infections, such as spontaneous bacterial peritonitis (SBP) or pneumonia, are frequent clinical complications and causes of death in patients with advanced cirrhosis [20], because in such immune-compromised patients the innate immune cells can not normally respond to the pathogen [21]. Neutrophils, macrophages, and DCs are important cellular mediators of the innate immune defense. Circulating monocytes, however, are increasingly implicated as essential players in the defense against a range of microbial pathogens [22]. Previously, we made two serum-free media (HCM and ACM) to examine more closely the actual amino acid environment of the living body plasma [9]. First, we showed that plasma L-Cys was increased by renal dysfunction, which is an important factor of the MELD score [18], and showed a significantly positive correlation with the monocyte counts in patient with advanced cirrhosis. However, high levels of L-Cys did not directly influence the proliferation of monocytes in vitro. This paradox raises the possibility that the GM-CSF from PBMCs (Fig. 2E) may indirectly increase the peripheral monocyte counts, because the increase is almost entirely due to the release from bone marrow [23]. This issue should be evaluated in future studies. Second, we showed that extracellular L-Cys dose-dependently increases pro-inflammatory cytokines from monocytes with LPS under the amino acid environment of patients with advanced cirrhosis. Concerning the mechanism that underlies these phenomena, we confirmed that high extracellular levels of L-Cys enhanced the exchange L-Cys/L-Glu antiport of monocytes via xCT, and decreased the intracellular GSH/GSSG ratio under the amino acid condition of advanced cirrhosis. A previous study showed that oxidized Eh L-Cysteine/L-Cys induces the upregulation of nuclear factor-kappa B of monocytes in vitro [24]. These studies support our results. However, the same studies reported that the oxidized extracellular Cys/CySS redox state had no effect on cellular GSH/GSSG redox [24,25]. We think that such differences were probably caused by differences in the culture condition and stimulation period of the immune cells, and that our culture conditions more closely matched the actual amino acid environment of patients with advanced cirrhosis. However, we need to investigate in detail by separate quantification of the reduced form, L-Cysteine; the oxidized form, L-Cys; and the mixed protein L-Cysteine disulfide. Furthermore, we think that a low level of plasma L-Glu enhances the antiport in patients with advanced cirrhosis, because another study reported on a L-Cys transport system whose activity was inhibited by L-Glu in mammalian cultured cells [26].

Finally, we confirmed that the TNF-alpha mRNA of CD14 monocytes, isolated from patients with advanced cirrhosis, was at a higher level than in healthy controls. Furthermore, the value of plasma TNF-alpha showed a significantly positive correlating with the plasma L-Cys/L-Glu ratio.

This present results still cannot be construed as conclusive evidence of a change in the immune system in patients with advanced cirrhosis. We need to investigate whether L-Cys/L-Glu imbalance influences other immune cells such as macrophages, dendritic cells, T-cells and B-cells, and their interaction, and whether the level of L-Glu influences the immune system, because previous studies reported that glutamate is a immunomediator in the intercellular cross-talk between DC and T cells [12,14,27]. In conclusion, we demonstrated for the first time that an L-Cys/L-Glu imbalance, especially high levels of L-Cys, increases pro-inflammatory cytokines, especially TNF-alpha from peripheral CD14+ monocytes under the amino acid condition of advanced cirrhosis in vitro, and these results are consistent with the relationships among plasma L-Cys and TNF-alpha in patients with advanced cirrhosis. This study may provide a new approach for future studies to ameliorate the immune dysfunction in patients with advanced cirrhosis.

Supporting Information

Figure S1 Linear regression model was used to model variation in plasma L-Cys and monocyte count. Among all twenty kinds of free amino acids, only L-Cys was significantly correlated with the monocyte counts in patients with advanced cirrhosis.
(TIF)

Table S1 The serum free culture media used in this study. 'ACM (advanced cirrhotic medium) consistent with the average concentration of plasma amino acids from patients (Child-Pugh grade B or C, n = 90). ACM+Cys: Varying concentrations of L-Cys were added to L-Cys-free ACM, and the final concentration was adjusted to 100–300 nmol/mL. ACM dep Cys: L-Cys free ACM. Other components except amino acids, were identical among media. The amino acid concentrations are expressed in nmol/mL. Fischer's ratio = (Valine+Leucine+Isoleucine)/(Tyrosine+Phenylalanine). We verified that there was no difference between the theoretical value and actual value examined by high performance liquid chromatography.
(DOC)

Table S2 Characteristics of study participants. LC-C: liver cirrhosis due to HCV LC-B: liver cirrhosis due to HBV HCC: hepatocellular carcinoma PBC: Primary biliary cirrhosis Alcoholic: Alcoholic cirrhosis NASH: non alcoholic steatohepatitis HA: Hepatic Encephalopathy PLT: platelet counts ($\times 10^3/\mu L$) PT-INR: prothrombin time-international normalized ratio AST/ALT: aspartate amino transferase/alanine amino transferase (IU/L) Total Bilirubin (mg/dL) Albumin (g/dL) Fischer's ratio mean: L-Valine+L-Leucine+L-Isoleucine/L-Tyrosine+L-Phenylalanine.
(DOC)

Acknowledgments

We thank Dr. Hideyo Sato (University of Yamagata) for thoughtful discussions and Sonoko Ishizaki (Ajinomoto Pharmaceuticals Co) for helpful suggestions. We thank Takeshi Sato (Cell Science & Technology Institute, Inc, Sendai, Japan.) for providing the high quality serum free media. We thank Chikako Sato for excellent technical assistance.

Author Contributions

Conceived and designed the experiments: EK YU YK JI MN KF TS. Performed the experiments: EK YK JI MN OK YW. Analyzed the data: EK YU KF KT TS. Contributed reagents/materials/analysis tools: EK YU YK JI MN. Wrote the paper: EK YU YK TS.

References

1. Tilg H, Wilmer A, Vogel W, Herold M, Nolchen B, et al. (1992) Serum levels of cytokines in chronic liver diseases. Gastroenterology 103: 264–274.
2. Byl B, Roucloux I, Crusiaux A, Dupont E, Deviere J (1993) Tumor necrosis factor alpha and interleukin 6 plasma levels in infected cirrhotic patients. Gastroenterology 104: 1492–1497.
3. Riordan SM, Skinner N, Nagree A, McCallum H, McIver CJ, et al. (2003) Peripheral blood mononuclear cell expression of toll-like receptors and relation to cytokine levels in cirrhosis. Hepatology 37: 1154–1164.
4. Ubeda M, Munoz L, Borrero MJ, Diaz D, Frances R, et al. (2010) Critical role of the liver in the induction of systemic inflammation in rats with preascitic cirrhosis. Hepatology 52: 2086–2095.
5. Navasa M, Follo A, Filella X, Jimenez W, Francitorra A, et al. (1998) Tumor necrosis factor and interleukin-6 in spontaneous bacterial peritonitis in cirrhosis: relationship with the development of renal impairment and mortality. Hepatology 27: 1227–1232.
6. Gines P, Schrier RW (2009) Renal failure in cirrhosis. N Engl J Med 361: 1279–1290.
7. Morgan MY, Marshall AW, Milsom JP, Sherlock S (1982) Plasma amino-acid patterns in liver disease. Gut 23: 362–370.
8. Kakazu E, Kanno N, Ueno Y, Shimosegawa T (2007) Extracellular branched-chain amino acids, especially valine, regulate maturation and function of monocyte-derived dendritic cells. J Immunol 179: 7137–7146.
9. Kakazu E, Ueno Y, Kondo Y, Fukushima K, Shiina M, et al. (2009) Branched chain amino acids enhance the maturation and function of myeloid dendritic cells ex vivo in patients with advanced cirrhosis. Hepatology 50: 1936–1945.
10. Walshe JM, Senior B (1955) Disturbances of cystine metabolism in liver disease. J Clin Invest 34: 302–310.
11. Lemberg A, Fernandez MA (2009) Hepatic encephalopathy, ammonia, glutamate, glutamine and oxidative stress. Ann Hepatol 8: 95–102.
12. Pacheco R, Oliva H, Martinez-Navio JM, Climent N, Ciruela F, et al. (2006) Glutamate released by dendritic cells as a novel modulator of T cell activation. J Immunol 177: 6695–6704.
13. Eck HP, Droge W (1989) Influence of the extracellular glutamate concentration on the intracellular cyst(e)ine concentration in macrophages and on the capacity to release cysteine. Biol Chem Hoppe Seyler 370: 109–113.
14. D'Angelo JA, Dehlink E, Platzer B, Dwyer P, Circu ML, et al. (2010) The cystine/glutamate antiporter regulates dendritic cell differentiation and antigen presentation. J Immunol 185: 3217–3226.
15. Sato H, Shiiya A, Kimata M, Maebara K, Tamba M, et al. (2005) Redox imbalance in cystine/glutamate transporter-deficient mice. J Biol Chem 280: 37423–37429.
16. Sato H, Tamba M, Ishii T, Bannai S (1999) Cloning and expression of a plasma membrane cystine/glutamate exchange transporter composed of two distinct proteins. J Biol Chem 274: 11455–11458.
17. Matsuo S, Imai E, Horio M, Yasuda Y, Tomita K, et al. (2009) Revised equations for estimated GFR from serum creatinine in Japan. Am J Kidney Dis 53: 982–992.
18. Kamath PS, Wiesner RH, Malinchoc M, Kremers W, Therneau TM, et al. (2001) A model to predict survival in patients with end-stage liver disease. Hepatology 33: 464–470.
19. Dennis PB, Jaeschke A, Saitoh M, Fowler B, Kozma SC, et al. (2001) Mammalian TOR: a homeostatic ATP sensor. Science 294: 1102–1105.
20. Gustot T, Durand F, Lebrec D, Vincent JL, Moreau R (2009) Severe sepsis in cirrhosis. Hepatology 50: 2022–2033.
21. Galbois A, Thabut D, Tazi KA, Rudler M, Mohammadi MS, et al. (2009) Ex vivo effects of high-density lipoprotein exposure on the lipopolysaccharide-induced inflammatory response in patients with severe cirrhosis. Hepatology 49: 175–184.
22. Serbina NV, Jia T, Hohl TM, Pamer EG (2008) Monocyte-mediated defense against microbial pathogens. Annu Rev Immunol 26: 421–452.
23. Van Furth R, Diesselhoff-den Dulk MC, Mattie H (1973) Quantitative study on the production and kinetics of mononuclear phagocytes during an acute inflammatory reaction. J Exp Med 138: 1314–1330.
24. Go YM, Jones DP (2005) Intracellular proatherogenic events and cell adhesion modulated by extracellular thiol/disulfide redox state. Circulation 111: 2973–2980.
25. Iyer SS, Accardi CJ, Ziegler TR, Blanco RA, Ritzenthaler JD, et al. (2009) Cysteine redox potential determines pro-inflammatory IL-1beta levels. PLoS One 4: e5017.
26. Bannai S, Kitamura E (1980) Transport interaction of L-cystine and L-glutamate in human diploid fibroblasts in culture. J Biol Chem 255: 2372–2376.
27. Fallarino F, Volpi C, Fazio F, Notartomaso S, Vacca C, et al. (2010) Metabotropic glutamate receptor-4 modulates adaptive immunity and restrains neuroinflammation. Nat Med 16: 897–902.

Am J Physiol Gastrointest Liver Physiol 301: G297–G305, 2011.
First published May 19, 2011; doi:10.1152/ajpgi.00418.2010.

Knockout of the neurokinin-1 receptor reduces cholangiocyte proliferation in bile duct-ligated mice

Shannon Glaser,[1,2,3] Eugenio Gaudio,[5] Anastasia Renzi,[2,5] Romina Mancinelli,[5] Yoshiyuki Ueno,[6] Julie Venter,[2,3] Mellanie White,[2,3] Shelley Kopriva,[2] Valorie Chiasson,[2] Sharon DeMorrow,[2,3] Heather Francis,[2,3,4] Fanyin Meng,[2,4] Marco Marzioni,[7] Antonio Franchitto,[5] Domenico Alvaro,[8] Scott Supowit,[9] Donald J. DiPette,[9] Paolo Onori,[10]* and Gianfranco Alpini[1,2,3]*

[1]Division of Research, Central Texas Veterans Health Care System, [2]Department of Medicine, [3]Scott & White Digestive Disease Research Center, and [4]Division of Research and Education, Scott & White and Texas A&M Health Science Center College of Medicine, Temple, Texas; [5]Department of Anatomical, Histological, Forensic Medicine and Orthopedics Sciences, University of Rome "La Sapienza," Rome, Italy; [6]Division of Gastroenterology, Tohoku University Graduate School of Medicine, Aobaku, Sendai, Japan; [7]Department of Gastroenterology, Università Politecnica delle Marche, Ospedali Riuniti General Hospital of Ancona, Italy; [8]Division of Gastroenterology, Department of Clinical Medicine, Polo Pontino, University of Rome, "Sapienza," Rome, Italy; [9]Division of Cell Biology and Anatomy, Medicine, University of South Carolina Medical School, Columbia, South Carolina; and [10]Experimental Medicine, University of L'Aquila, L'Aquila, Italy

Submitted 16 September 2010; accepted in final form 6 May 2011

Glaser S, Gaudio E, Renzi A, Mancinelli R, Ueno Y, Venter J, White M, Kopriva S, Chiasson V, DeMorrow S, Francis H, Meng F, Marzioni M, Franchitto A, Alvaro D, Supowit S, DiPette DJ, Onori P, Alpini G. Knockout of the neurokinin-1 receptor reduces cholangiocyte proliferation in bile duct-ligated mice. *Am J Physiol Gastrointest Liver Physiol* 301: G297–G305, 2011. First published May 19, 2011; doi:10.1152/ajpgi.00418.2010.—In bile duct-ligated (BDL) rats, cholangiocyte proliferation is regulated by neuroendocrine factors such as α-calcitonin gene-related peptide (α-CGRP). There is no evidence that the sensory neuropeptide substance P (SP) regulates cholangiocyte hyperplasia. Wild-type (WT, $^{+/+}$) and NK-1 receptor (NK-1R) knockout (NK-1R$^{-/-}$) mice underwent sham or BDL for 1 wk. Then we evaluated *1*) NK-1R expression, transaminases, and bilirubin serum levels; *2*) necrosis, hepatocyte apoptosis and steatosis, and the number of cholangiocytes positive by CK-19 and terminal deoxynucleotidyl transferase biotin-dUTP nick-end labeling in liver sections; *3*) mRNA expression for collagen 1α and α-smooth muscle (α-SMA) actin in total liver samples; and *4*) PCNA expression and PKA phosphorylation in cholangiocytes. In cholangiocyte lines, we determined the effects of SP on cAMP and D-myo-inositol 1,4,5-trisphosphate levels, proliferation, and PKA phosphorylation. Cholangiocytes express NK-1R with expression being upregulated following BDL. In normal NK-1R$^{-/-}$ mice, there was higher hepatocyte apoptosis and scattered hepatocyte steatosis compared with controls. In NK-1R $^{-/-}$ BDL mice, there was a decrease in serum transaminases and bilirubin levels and the number of CK-19-positive cholangiocytes and enhanced biliary apoptosis compared with controls. In total liver samples, the expression of collagen 1α and α-SMA increased in BDL compared with normal mice and decreased in BDL NK-1R$^{-/-}$ compared with BDL mice. In cholangiocytes from BDL NK-1R $^{-/-}$ mice there was decreased PCNA expression and PKA phosphorylation. In vitro, SP increased cAMP levels, proliferation, and PKA phosphorylation of cholangiocytes. Targeting of NK-1R may be important in the inhibition of biliary hyperplasia in cholangiopathies.

biliary epithelium; cAMP; innervation; mitosis; sensory innervation

HUMAN CHOLANGIOCYTES ARE THE target cells in a number of cholestatic liver diseases (i.e., cholangiopathies) including primary sclerosing cholangitis and primary biliary cirrhosis (5, 28), which are characterized by an abnormal balance between biliary growth and damage (5, 28). In animal models of cholestasis, changes in biliary growth and damage are achieved by a number of pathophysiological maneuvers including extrahepatic bile duct ligation (BDL) (4, 15, 23), acute administration of carbon tetrachloride (CCl_4) (31), cholinergic (30) denervation, and ablation of sensory innervation by knockdown of α-calcitonin gene-related peptide (α-CGRP) (23). In these models, small and large cholangiocytes (lining small and large bile ducts, respectively) (2, 6, 21) show a different biological response, in terms of proliferation, survival, and secretory activity (3, 15, 21, 30, 31). Relevant to this study, in the cholestatic BDL rodent model large but not small cholangiocytes undergo mitosis leading to enhanced large bile duct mass (3, 15, 31). Two second messengers, D-myo-inositol 1,4,5-trisphosphate (IP_3) and cyclic adenosine 3′,5′-monophosphate (cAMP), regulate the proliferative, apoptotic, and secretory functions of small and large cholangiocytes (3, 15–17, 23, 30, 31). Although the IP_3/Ca^{2+}-dependent signaling modulates the function of small cholangiocytes (16, 31), large cholangiocyte hyperplasia following BDL is regulated by the activation of cAMP-dependent PKA signaling (3, 15, 17, 23, 30).

Two afferent nerve pathways are present in the liver: the vagal and the spinal afferent nerve pathways that run through the dorsal root ganglion (45). Sensory nerves also display an efferent function, which is mediated by the release of sensory neuropeptides such α-CGRP from their peripheral terminals in tissues that they innervate modulating cellular functions (25). Substance P (SP), containing peptidergic nerves, is present in the spinal afferent nerve pathway. SP-positive innervation has been localized in the periportal regions of guinea pig and human liver (43). SP is a member of the tachykinin peptide family that is formed by six members: SP, neurokinin A, neurokinin B, neuropeptide K, neuropeptide γ, and hemokinin (1). SP and neurokinin A are present in the central nervous system and primary sensory afferent neurons innervating peripheral tissues and are released from sensory nerve endings both at the level of the spinal cord and in peripheral tissues (1). The tachykinin receptor family consists of three types of seven transmembrane G protein-coupled receptors: neurokinin-1, -2,

* P. Onori and G. Alpini share the last authorship.
Address for reprint requests and other correspondence: G. Alpini, Central Texas Veterans Health Care System and Digestive Disease Research Center and Texas A&M Health Science Center College of Medicine, 702 SW H. K. Dodgen Loop, Temple, TX, 76504 (e-mail: galpini@tamu.edu or galpini@medicine.tamhsc.edu).

0193-1857/11 Copyright © 2011 the American Physiological Society

and -3 receptors (NK-1R, NK-2R, and NK-3R). SP preferentially binds and signals via the NK-1R (1). Limited data exist regarding the role of sensory innervation in the regulation of biliary functions. Tachykinins are the main nonadrenergic and noncholinergic excitatory neurotransmitters in the common bile duct of guinea pigs (38). Sensory neuropathy has been associated in patients with primary biliary cirrhosis (13). Also, knockout of α-CGRP reduces cholangiocyte hyperplasia in cholestatic BDL mice by downregulation of cAMP signaling (23). No data exist regarding the role of SP in the regulation of biliary hyperplasia during cholestasis induced by BDL.

In many cell types, SP-induced activation of NK-1R (coupled to pertussis toxin-insensitive G_q/G_{II}) activates phospholipase C and subsequent formation of IP_3 and diacylglycerol mobilizing intracellular Ca^{2+} (26, 36). In other cells (27, 37), NK-1R also couple to *1*) $G\alpha_s$ resulting in adenylyl cyclase activation (37) and cAMP formation and *2*) $G\alpha_i$ that inhibits cAMP formation. On the basis of this background, we aim to demonstrate that SP and its receptor, NK-1R, regulate the proliferation of cAMP-dependent large cholangiocytes in the cholestatic BDL mouse model.

MATERIALS AND METHODS

Materials. Reagents were purchased from Sigma Chemical (St. Louis, MO) unless otherwise indicated. The nuclear dye 4,6-diamidino-2-phenylindole (DAPI) was obtained from Molecular Probes, Eugene, OR. The NK-1R antibody against the rat COOH-terminal (393–407) peptide was purchased from Enzo Life Sciences International (Plymouth Meeting, PA). SP was purchased from Phoenix Pharmaceuticals (Burlingame, CA). The antibody against proliferating cell nuclear antigen (PCNA) was purchased from Santa Cruz Biotechnology (Santa Cruz, CA). The mouse anti-cytokeratin-19 (CK-19) antibody (clone RCK105) was purchased from Caltag Laboratories (Burlingame, CA). The cAMP-dependent phospho-PKA catalytic subunit (Thr197) antibody (Cell Signaling, Boston, MA) detects endogenous levels of PKA catalytic subunit (-α, -β, and -γ) only when phosphorylated at Thr197. The cAMP-dependent PKA catalytic subunit-α antibody (Cell Signaling) detects endogenous levels of total PKA catalytic subunit-α. The antibodies for the rabbit anti-ERK1 (which detects p44 and p42) and goat anti-pERK (which detects phosphorylated p44 and p42) were purchased from Santa Cruz Biotechnology RIA kits for the determination of cAMP and IP_3 levels were purchased from GE Healthcare (Arlington Heights, IL).

Animal models. The majority of the studies were performed in wild-type (WT, $^{+/+}$) and NK-1R knockout (NK-1R $^{-/-}$) normal (sham-operated) and 1-wk BDL mice (Table 1); since we did not see

Table 1. *Evaluation of NK-1R expression, liver and body weight, liver-to-body weight ratio in the selected groups of animals*

Groups	NK-1R Expression	Liver Weight, g	Body Weight, g	Liver/body weight × 100, %
WT normal mice (n = 84)	(−/+)	1.98 ± 0.05	26.3 ± 0.5	7.58 ± 0.16
NK-1R$^{-/-}$ normal mice (n = 79)	(−)	1.80 ± 0.05	28.3 ± 0.7	6.25 ± 0.18*
WT BDL mice (n = 41)	(++)	1.94 ± 0.06	21.92 ± 0.3†	8.84 ± 0.21†
NK-1R$^{-/-}$ BDL mice (n = 25)	(−)	2.07 ± 0.09	25.9 ± 0.7‡	7.96 ± 0.27‡

Data are means ± SE. ND, not detectable; NK-1R, neurokinin-1 receptor. *, †$P < 0.05$ vs. the corresponding value of normal wild-type (WT) mice. ‡$P < 0.05$ vs. the corresponding value of WT bile duct-ligated (BDL) mice.

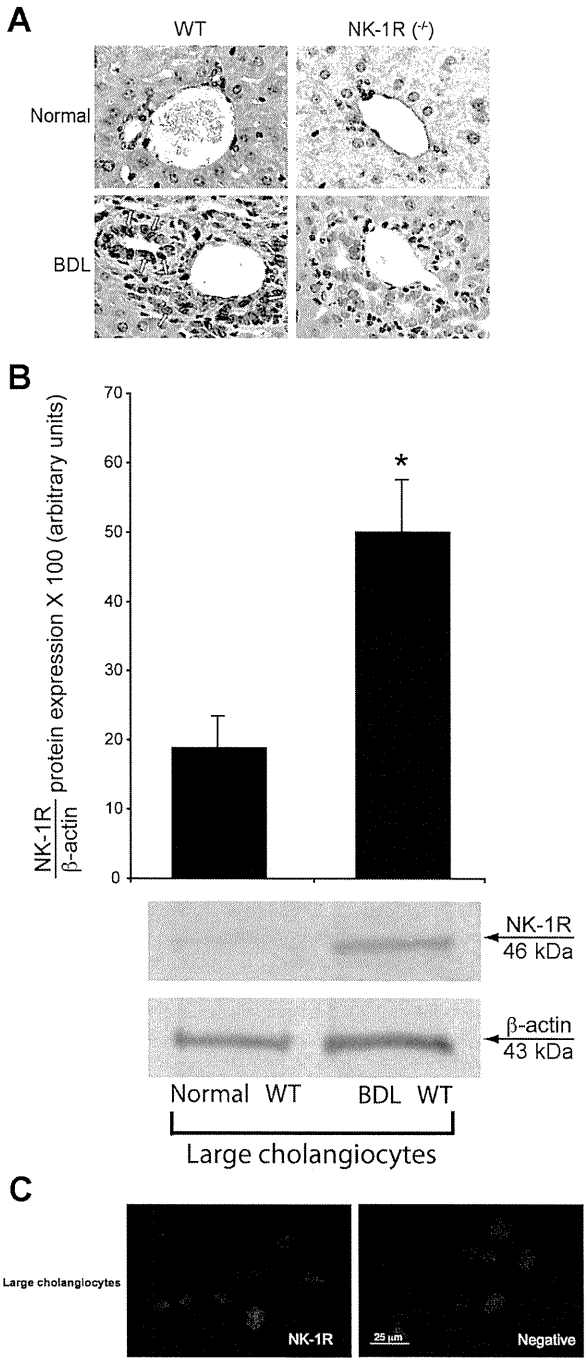

Fig. 1. *A*: expression of NK-1 receptor (NK-1R) was low in bile ducts from normal wild-type (WT; red arrow) mice but increased in bile ducts from bile duct-ligated (BDL) WT mice (yellow arrows; see Table 1). NK-1R was absent in intrahepatic bile ducts from normal and BDL NK-1R knockout (NK-1R$^{-/-}$) mice. Original magnification ×40. *B*: protein expression of NK-1R increased in large cholangiocytes from BDL WT mice compared with large cholangiocytes from normal WT mice. Data are means ± SE of 6 immunoblots derived from protein obtained from cumulative preparations of cholangiocytes. *$P < 0.05$ vs. the corresponding value of BDL large cholangiocytes. *C*: specific immunoreactivity for NK-1R in representative fields of large cholangiocytes is shown in red; cell nuclei were stained with 4,6-diamidino-2-phenylindole (DAPI; blue). Bar size = 25 μm.

Table 2. *Evaluation of serum levels of transaminases and bilirubin*

Groups	Alanine Aminotransferase, units/l	Aspartate Aminotransferase, units/l	Total Bilirubin, mg/l
WT normal mice	20.2 ± 2.4 (n = 8)	55.2 ± 3.9 (n = 8)	<0.1 (n = 8)
NK-1R$^{-/-}$ normal mice	123.8 ± 20.7 (n = 11)	229.3 ± 23.2 (n = 12)	<0.1 (n = 16)
WT BDL mice	687.1 ± 119.1* (n = 6)	1,134.6 ± 212.1* (n = 5)	13.58 ± 1.74* (n = 7)
NK-1R$^{-/-}$ BDL mice	389 ± 35† (n = 6)	708.6 ± 50.6† (n = 5)	9.22 ± 1.1† (n = 7)

Data are means ± SE of 7 evaluations. *P < 0.05 vs. the corresponding value of normal WT mice. †P < 0.05 vs. the corresponding value of WT mice with BDL for 7 days.

any difference in biliary growth between normal and sham-operated mice (not shown), we used normal mice in our studies. Some of the experiments were also performed in normal and 1-wk BDL heterozygous mice (derived from the same breeding) to evaluate hepatocyte apoptosis and steatosis, lobular necrosis, the degree of inflammation and intrahepatic bile duct mass, and biliary apoptosis in vivo. BDL was performed as described (22, 23, 35). The NK-1R$^{-/-}$ mouse model (25–30 g, of the N5 generation) is bred at our Animal Facility; the original breeding pair was a gift from Dr. Norma Gerard (Harvard Medical School, Boston, MA) to Dr. Donald DiPette (coauthor in this article). This is a homozygous$^{-/-}$ model on a C57BL/6 background. The mouse model lacking the NK-1R gene was generated as described (12). Age-matched male C57BL/6 wild-type (WT) mice were purchased from Charles River (Wilmington, MA), whereas heterozygous mice were obtained from our breeding colony. All mice were maintained in a temperature-controlled environment (20–22°C) with 12: 12-h light-dark cycles. Before each experimental procedure, animals were injected with pentobarbital sodium (50 mg/kg body wt ip). All animal experiments were performed according to a protocol approved by the Scott and White and Texas A&M Health Science Center Institutional Animal Care and Use Committee.

Immortalized and freshly isolated large cholangiocytes. Since BDL induces the proliferation of large but not small cholangiocytes (21, 23), the signaling studies were performed in freshly isolated large cholangiocytes from WT and NK-1R$^{-/-}$ BDL mice, and our immortalized line of large cholangiocytes, which display phenotypical and functional characteristics similar to those of freshly isolated large cholangiocytes (16, 21, 22). Virtually pure (by CK-19 immunohistochemistry) (16) isolated large cholangiocytes were obtained by centrifugal elutriation followed by immunoaffinity separation (16, 21) by using a monoclonal antibody, mouse IgG2a (provided by Dr. R. Faris, Providence, RI) against an antigen expressed by all intrahepatic cholangiocytes (21).

Evaluation of NK-1R protein expression. Analysis of NK-1R expression was evaluated by semiquantitative immunohistochemistry in paraffin-embedded liver sections (4–5 μm; 6 slides per treatment group; for each slide 6 nonoverlapping fields were evaluated) (16, 21) from the selected groups of animals. Following immunohistochemistry, photographs of liver sections were taken by Leica Microsystems DM 4500 B Light Microscopy (Weltzlar, Germany) with a Jenoptik Prog Res C10 Plus Videocam (Jena, Germany). The quantitative expression of NK-1R was measured by immunoblots (16) in protein (10 μg) from whole cell lysate from large cholangiocytes from normal and BDL WT mice. The intensity of the bands was determined by scanning video densitometry using the phospho-imager Storm 860 and the ImageQuant TL software version 2003.02 (GE Healthcare, Little Chalfont, Buckinghamshire, UK). The presence of NK-1R was also evaluated by immunofluorescence (14, 16) in immortalized large cholangiocytes. Images were visualized via an Olympus IX-71 confocal microscope. For all immunoreactions, negative controls (with normal serum from the same species substituted for the primary antibody) were included.

Evaluation of serum levels of transaminases and bilirubin, lobular necrosis, inflammation, hepatocyte apoptosis and steatosis, and cholangiocyte proliferation and apoptosis. In the in vivo studies, we measured *1*) liver weight, body weight, and liver-to-body weight ratio (4) and *2*) serum levels of transaminases, alanine aminotransferase and aspartate aminotransferase, and total bilirubin using a Dimension RxL Max Integrated Chemistry system (Dade Behring, Deerfield IL) by the Chemistry Department, Scott & White.

We evaluated *1*) lobular necrosis and the degree of inflammation by hematoxylin and eosin (H&E) staining; *2*) the percentage of apoptotic hepatocytes by terminal deoxynucleotidyl transferase biotin-dUTP nick-end labeling (TUNEL) kit (33) (Apoptag; Chemicon International); and *3*) the number of large cholangiocytes (lining large bile ducts, > 15 μm diameter) (2) positive for PCNA (15) and CK-19 (39) or by TUNEL kit (33) in liver sections (4–5 μm; 6 slides per treatment group; for each slide 6 nonoverlapping fields were evaluated) from the selected groups of animals. The degree of hepatocyte steatosis was evaluated in frozen liver sections (4–5 μm thick) by both H&E staining and the oil red O staining kit (32) (IHC World, Woodstock, MD). All sections were examined in a coded fashion by two board certified pathologists by a BX-51 light microscope (Olympus, Tokyo, Japan) equipped with a camera. We also evaluated the damage of a number of tissues/organs in the experimental groups listed in Table 1.

Evaluation of gene expression for collagen 1α and α-smooth muscle actin in total liver samples. We measured the expression of the messages for collagen 1α and α-smooth muscle actin (α-SMA) in RNA (0.5 μg) in total liver tissue by the RT^2 Real-Time assay from SABiosciences (Frederick, MD) (16). A $\Delta\Delta C_T$ (delta delta of the threshold cycle) analysis was performed by using RNA from normal WT mice as the control sample. Data were expressed as relative mRNA levels ± SE of the selected gene-to-GAPDH ratio. The primers for collagen 1α and α-SMA (purchased from SABiosciences) were designed according to the NCBI GenBank Accession numbers: NM_007742 (for collagen 1α) (18) and NM_007392 (for α-SMA) (34).

Measurement of PCNA protein expression and phosphorylation of PKA in purified large cholangiocytes. In protein (10 μg) from whole cell lysate from spleen (positive control) and purified large cholangiocytes from WT and NK-1R$^{-/-}$ BDL mice, we evaluated by immunoblots (16, 21) cholangiocyte proliferation by PCNA protein expression (measured as ratio to β-actin protein expression) (16), and the phosphorylation of cAMP-dependent PKA (expressed as ratio to protein expression of the corresponding total protein), a molecule playing an important role in cAMP-dependent regulation of large cholangiocyte proliferation (8, 15, 17). The intensity of the bands was determined by scanning video densitometry using the phospho-imager

Table 3. *Evaluation of the percentage of hepatocytes positive by TUNEL*

Groups	Percentage of Hepatocytes Positive by TUNEL
WT normal mice	4.2 ± 0.44
NK-1R$^{-/-}$ normal mice	4.9 ± 0.48*
WT 7 BDL mice	31.8 ± 2.3*
NK-1R$^{-/-}$ BDL mice	34.0 ± 2.6

Data are means ± SE. TUNEL, terminal deoxynucleotidyltransferase biotin-dUTP nick-end labeling. *P < 0.05 vs. the corresponding value of normal WT mice.